Received: 21 August 2020 | Revised: 2 February 2021 | Accepted: 14 February 2021

DOI: 10.1111/jzs.12470

JOURNAL OF ZOOLOGICAL SYSTEMATICS AND EVOLUTIONARY RESEARCH — WILEY

ORIGINAL ARTICLE

Genetically diverse yet morphologically conserved: Hidden diversity revealed among Bornean geckos (Gekkonidae: *Cyrtodactylus*)

Hayden R. Davis[1,2] | **Indraneil Das**[3] | **Adam D. Leaché**[1] | **Benjamin R. Karin**[4] | **Ian G. Brennan**[5] | **Todd R. Jackman**[2] | **Izneil Nashriq**[3] | **Kin Onn Chan**[6] | **Aaron M. Bauer**[2]

[1]Department of Biology, Burke Museum of Natural History and Culture, University of Washington, Seattle, WA, USA

[2]Department of Biology, Center for Biodiversity and Ecosystem Stewardship, Villanova University, Villanova, PA, USA

[3]Institute of Biodiversity and Environmental Conservation, Universiti Malaysia Sarawak, Kota Samarahan, Malaysia

[4]Department of Integrative Biology, Museum of Vertebrate Zoology, University of California, Berkeley, CA, USA

[5]Division of Ecology and Evolution, Research School of Biology, The Australian National University, Canberra, ACT, Australia

[6]Lee Kong Chian Natural History Museum, National University of Singapore, Singapore

Correspondence
Hayden R. Davis, Department of Biology, Burke Museum of Natural History and Culture, University of Washington, Seattle, WA 98195, USA.
Email: hrdavis1@uw.edu

Funding information
Lee Kong Chian Natural History Museum Collection Study Grant; The Society of Integrative and Comparative Biology; Museum of Comparative Zoology, Harvard University; Gerald M. Lemole Endowed Chair Fund; Government of Malaysia, Grant/Award Number: (NRGS/1087/2013(01)

Abstract

The appreciation of cryptic biological diversity, and the pace at which it is recognized, has greatly increased with the use of molecular systematic techniques. The gekkonid genus *Cyrtodactylus* Gray, 1827 is one example of a group that has undergone a particularly rapid increase in recognized diversity due to molecular systematic studies. Many of these new species result from recognizing closely related but diagnosable lineages into sister taxa. Our study implements a multi-faceted approach to delimit cryptic *Cyrtodactylus* lineages on the Southeast Asian island of Borneo using morphological, ecological, and multilocus genetic data. We use multiple species delimitation models to assess species boundaries and identify clades that warrant further investigation. Unlike most morphologically cryptic species that have recently diverged, we find evidence of cryptic lineages being polyphyletic. Using multivariate statistical analyses, we show minimal phenotypic distinction between putative cryptic species within the *C. pubisulcus* complex. Despite not finding morphologically diagnostic characters, we demonstrate strong evidence for the specific recognition of *C. hantu* sp. nov. and *C. miriensis* sp. nov., which are currently considered conspecific with *C. pubisulcus*, from Sarawak, Malaysia. Our new concept for *C. pubisulcus* restricts the geographic range of the species to specific regions in western Sarawak, Malaysia, thus underscoring the need to conserve the limited remaining habitats of these species, as well as the considerable undescribed diversity across Borneo.

KEYWORDS
ancestral state reconstruction, cryptic species, new species, species delimitation, Squamata

Zoobank link:LSID: urn:lsid:zoobank.org:pub:D318F944-1194-4011-A145-EA45415A3DAD **Online ISSN: 1439-0469**

1 | INTRODUCTION

Recognizing extant species diversity is crucial for the implementation of well-informed conservation practices, yet biodiversity inventories are often incomplete because they rely on species lists that often overlook lineages with similar morphologies. The incorporation of genetic data into systematic studies has greatly increased the amount of recognized biodiversity by detecting morphologically indistinguishable (cryptic) species (Pfenninger & Schwenk, 2007). Members of cryptic herpetofaunal clades revealed using molecular phylogenetic methods have been subsequently differentiated using a variety of approaches, including pheromones (Zozaya et al., 2019), vocalization patterns (Channing et al., 2002; Funk et al., 2012), larval differences (Hebert et al., 2004), hybrid incompatibility (Corl et al., 2012), or behavioral characteristics (Montanarin et al., 2011), among others. Further, some taxa that could not be distinguished using traditional morphological data (e.g., meristic, 2-D morphometrics, coloration, etc.) have been differentiated using 3-D geometric morphometrics (Chaplin et al., 2020). These studies reinforce the best practices for delimiting morphologically similar species using a broad combination of data, including morphology and molecular genetic data, and natural history information.

Many recently described species are termed "cryptic" leading to confusion over what constitutes a cryptic species. The first clear explanation of the term was presented by Mayr (1976) in reference to species that were superficially indistinguishable based on morphology, ranging from ants with the presence of hairs on particular anatomical structures, to structurally identical wasps that varied in color pattern. As molecular genetic data has become more readily accessible for taxonomic studies, a rise in the number of cryptic species has ensued leading to varying viewpoints as to what "cryptic" refers (Bickford et al., 2007). Multiple empirical and review-based studies have provided formal definitions for cryptic species (Bickford et al., 2007; Fišer et al., 2018; Singhal et al., 2018; Struck et al., 2018), yet the definitions provided continue to be debated (Heethoff, 2018; Korshunova et al., 2019). As a result, empirical examples of cryptic species encompass a broad morphological spectrum, with some species showing distinct (Koch et al., 2009; Lobo & Espinoza, 1999), subtle (Grismer et al., 2013; Oliver et al., 2020), or absence of (Pepper et al., 2011; Singhal & Moritz, 2013) diagnostic phenotypic characters. This raises the question—when should the broadly used term "cryptic" be applied to a species?

We consider species to be cryptic if they depend on additional sources of data to formulate the delineation hypothesis prior to establishing diagnostic morphological characters. This definition of cryptic species includes those that would require a microscope, or other means of deeper investigation, to determine their species assignment, or those for which morphological diagnostics are realized only after molecular genetic data are available (Stuart et al., 2006). Such species could ultimately be differentiated with a more thorough examination of morphological (i.e., slight variation in discrete characters or morphometric data, etc.), behavioral, ecological, physiological, or geographic distributional data. We find this interpretation of the term is more closely aligned with the original essence of the proposal by Mayr (1976).

We apply this definition of cryptic species to study the highly diverse gekkonid genus *Cyrtodactylus* Gray, 1827. The genus spans from South Asia to northern Australia and has seen an increased focus on taxonomic work, leading to nearly 200 descriptions in the past decade, making it the most species-rich genus of geckos in the world (Brennan et al., 2017; Uetz, 2020). Genetic data demonstrated that many wide-ranging taxa comprised genetically distinct groups, with many species being referred to as cryptic (Agarwal & Karanth, 2015; Agarwal et al., 2018; Grismer et al., 2012, 2014, 2016, 2018; Luu et al., 2016; Murdoch et al., 2019; Nazarov, Orlov, Sang, & Cuc, 2008, 2012; Nguyen et al., 2017; Oliver et al., 2012, 2018; Ziegler et al., 2010). These molecular-based systematic studies have been instrumental in uncovering hidden diversity, but the Southeast Asian island of Borneo has only recently been investigated (Davis et al., 2019, 2020). Due to the prior lack of molecular genetic studies on Borneo, only 10 species of *Cyrtodactylus* are currently recognized, nine of which are endemic. Borneo is the third largest island in the world and encompasses a geographic area roughly three times that of Peninsular Malaysia. Although Borneo and Peninsular Malaysia shared a recent terrestrial connection (Sarr et al., 2019), Peninsular Malaysia has nearly four times the recognized *Cyrtodactylus* diversity (Grismer & Quah, 2019), which suggests that Bornean *Cyrtodactylus* diversity may be substantially higher. The recent studies targeting the diversity of Bornean *Cyrtodactylus* highlighted the high amount of diversity on the island with multiple undescribed cryptic lineages and high intraspecific genetic diversity (Davis et al., 2019, 2020).

Cyrtodactylus pubisulcus Inger, 1958 is a relatively small-bodied (maximum snout-vent length [SVL] ~75 mm) gecko with a type locality of Gunung Matang, Sarawak, Malaysia (Inger, 1961; Figure 1), which almost exclusively occurs on bushes and other low vegetation in primary and secondary rainforests. *Cyrtodactylus pubisulcus* is endemic to Borneo (Hikida, 1990), and previous records indicated that *C. pubisulcus* was wide-ranging throughout Sarawak, the southern portion of Sabah, and the Nation of Brunei (Ahmad et al., 2019; Das, 2005, 2006, 2007; Das et al., 2008; Hikida, 1990; Inger & Tan, 2010). However, Davis et al. (2020) showed that morphospecies attributed to *C. pubisulcus* were phylogenetically polyphyletic, with distinct lineages in western (type locality), central, and eastern Sarawak. We herein refer to the western lineage as *C. pubisulcus* sensu stricto (*s.s.*), while the central and eastern lineages are referred to the by the geologic structural zone from which they occur: Sibu and Miri, respectively (Haile, 1974; Hutchinson, 2005). These three clades have deep genetic divergences with intrapopulation-level color variation and shared ecologies, leading to taxonomic confusion among and within the groups. A high amount of genetic diversity was revealed within *C. pubisulcus s.s.* with upwards of 10% pairwise divergence (*p*-distance) for the mitochondrial ND2 locus; and upwards of 9% *p*-distance within *C.* sp. nov. Miri (Davis et al., 2020). In addition, chromosomal differences are present between *C. pubisulcus s.s.* and *C.* sp. nov. Miri, with *C. pubisulcus s.s.* having metacentric chromosomes and *C.* sp. nov. Miri having a pair of subtelocentric

chromosomes (Ota et al., 1992). Accurately delineating these lineages and reassessing the taxonomy of *C. pubisulcus* is imperative to better estimate Borneo's biodiversity.

In this study, we present a case of cryptic speciation in which morphologically indistinguishable lineages form deeply divergent, polyphyletic groups. We investigate the boundaries within putative species using morphological data and DNA-based species delimitation analyses to determine whether *C. pubisulcus* warrants being split into multiple distinct species. We also incorporated multivariate statistical analyses to assess whether the polyphyletic lineages comprising *C. pubisulcus* are morphologically cryptic. Combining these results, we provide specific recognition to the Sibu and Miri clades of the *C. pubisulcus* complex based primarily on their deeply divergent phylogenetic relationship and disjunct geographic localities.

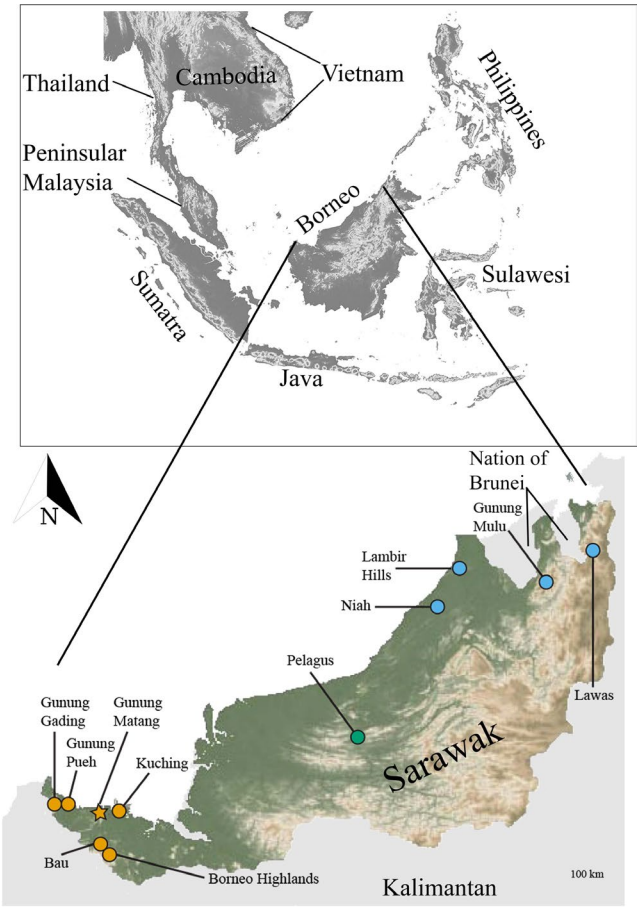

FIGURE 1 Upper map: Southeast Asia, indicating the position of Borneo. Lower map: Sarawak, Malaysia with the sampling localities noted by circles; the star represents the type locality of *Cyrtodactylus pubisulcus*. Colored circles indicate the geographic localities of the genetic material used in this study. Yellow circles = *C. pubisulcus sensu stricto*; green circles = *C. hantu* sp. nov.; and blue circles = *C. miriensis* sp. nov.

2 | MATERIALS AND METHODS

For this study, we collected both morphological and genetic data for the *C. pubisulcus* complex, which we compared to publicly available data. In total, we collected morphological data from 59 individuals and generated 35 targeted sequences. We collected all morphological data for species in the *C. pubisulcus* complex over the course of this study and compared our dataset to the morphological data of Davis et al. (2019). We generated 31 new genetic sequences (GenBank: MW197105–MW197131; MW258659–MW258662) and combined them with additional samples from GenBank (Table S1).

2.1 | Specimen collection

We conducted fieldwork in Sarawak, Malaysia, Borneo (Figure 1) over the years 2014–2018, chiefly during the months of May through July from the hours of 20:00 to 00:00. We euthanized individuals using a 1% MS-222 solution (Conroy et al., 2009; IACUC: 1864), preserved them using 10% formalin, and subsequently transferred them to 70% ethanol for long-term preservation. Vouchered specimens were either deposited at the California Academy of Sciences (CAS), San Francisco, CA, USA, the Institue of Biodiverstiy and Environmental Conservation, Universiti Malaysia Sarawak (UNIMAS), or are pending deposition with the Sarawak Forest Department, Kuching, Sarawak, MY. Tissue samples are stored at Villanova University, Villanova, PA and the University of Washington, Seattle, WA, USA.

TABLE 1 Primer sequences used for DNA amplification and sequencing, and the annealing temperatures used for PCR

Primer name	Primer design	Primer sequence: 5′–3′	Annealing temperature
ND2-METF1	Macey et al. (1997)	'AAGCTTTCGGGCCCATACC'	50°C
COI-R1	Macey et al. (1997)	'AGRGTGCCAATGTCTTTGTGRTT'	50°C
RAG1-SQAF396	Skipwith et al. (2016)	'TTKCTGAATGGAAATTCAAGCTSTT'	50°C
RAG1-397	Groth and Barrowclough (1999)	'GATGCTGCCTCGGTCGGCCACCTTT'	50°C
PDC-PHOF1	Bauer et al. (2007)	'AGATGAGCATGCAGGAGTATGA'	50° C
PDC-PHOR1	Bauer et al. (2007)	'TCCACATCCACAGCAAAAAACTCCT'	50°C
MXRA5-F2	Portik et al. (2012)	'KGCTGAGCCTKCCTGGGTGA'	55° C
MXRA5-R2	Portik et al. (2012)	'YCTMCGGCCYTCTGCAACATTK'	55°C

2.2 | Molecular genetic data

We isolated genomic DNA from liver or tail tips stored in 95% ethanol, using the extraction protocol described in Aljanabi and Martinez (1997). We amplified one mitochondrial protein coding gene and its flanking tRNAs: NADH dehydrogenase subunit 2 (*ND2*); and three protein coding nuclear loci: matrix remodeling associated 5 (*MXRA5*), recombination activating gene (*RAG1*), and phosducin gene (*PDC*) using a double-stranded polymerase chain reaction (PCR). The specific primers used for DNA amplification, along with their respective annealing temperatures and sequences, are shown in Table 1. The PCR products were about 1450 bp, 960 bp, 445 bp, and 1060 bp, respectively. After sequencing and trimming, the alignments for the new sequences were: 1374 bp, 865 bp, 442 bp, and 939 bp for *ND2*, *MXRA5*, *PDC*, and *RAG1*, respectively. More detailed sequencing protocols are outlined in Davis et al. (2019, 2020).

We assembled and aligned new sequences with GenBank sequences using the MAFFT algorithm in the program Geneious® v11.1.2 (Katoh & Standley, 2013; Kearse et al., 2012). Each gene was aligned individually and subsequently concatenated. The full concatenated dataset included 100 individuals spanning 40 species and 3907 bp [*ND2*: 1502 bp; *RAG1*: 1039 bp; *MXRA5*: 924 bp; *PDC*: 443 bp]. Our dataset includes most sequences in Davis et al. (2020), with an additional 27 new sequences spanning three taxonomic groups (*C. pubisulcus s.s.*, *C.* sp. nov. Sibu, and *C.* sp. nov. Miri; Table S1; Alignment S1).

2.3 | Phylogenetic analyses

We first inferred phylogenetic relationships using maximum likelihood (ML). To reconstruct ML phylogenies, we used IQ-TREE (Nguyen et al., 2015) implementing 5000 ultrafast bootstrap (UFB) replicates (Hoang et al., 2017); nodes with UFB values of 95 or higher were considered highly supported (Minh et al., 2013). We partitioned the dataset by gene and used ModelFinder to determine the best-fit evolutionary model for each gene (Kalyaanamoorthy et al., 2017). The evolutionary model selected for each gene was as follows: *ND2* − TIM + F + R4; *PDC* − TNe + I; *MXRA5* − HKY + F + R2; and *RAG1* − HKY + F + R2.

To assess gene tree discordance, we analyzed loci individually and concatenated. We estimated gene trees using IQ-TREE for *ND2*, *MXRA5*, and *RAG1*. Due to the slow rate of evolution for *PDC* and associated lack of phylogenetic resolution, we did not include the single-locus dataset in this study. To assess the relationships inferred from the nuclear loci, we concatenated *MXRA5*, *RAG1*, and *PDC*.

Due to the poor support at the deeper nodes and the slightly non-concordant topologies estimated in Davis et al. (2020), we also inferred the phylogenetic position of the two new species using a Bayesian approach. To estimate the Bayesian phylogeny, we used BEAST2 v.2.5.2 (Bouckaert et al., 2019) with the mitochondrial + nuclear concatenated dataset. We followed the methodology in Davis et al. (2020). We considered nodes with a posterior probability of 0.95 or above highly supported. To determine the pairwise distances for both the mitochondrial and nuclear loci, we used Geneious® v11.1.2.

2.4 | Species delimitation

We tested species delimitation models to assess the support of three distinct *C. pubisulcus* clades and to determine if additional populations warrant further delineation. Davis et al. (2020) conducted a preliminary species delimitation using Automatic Barcode Gap Discovery (ABGD; Puillandre et al., 2012). In our study, we present four additional species delimitation models to assess whether delimitation results are consistent between models because certain approaches underestimate true species diversity and others overestimate (Carstens et al., 2013). We used the General Mixed Yule Coalescent (GMYC) model (Fujisawa & Barraclough, 2013), the Bayesian Poisson Tree Process (bPTP) model (Zhang et al., 2013), and ABGD. Other than ABGD, all of the models require an input tree, for which we used the mitochondrial ML topology due to incomplete taxonomic coverage for the other loci, and to maintain consistency between analyses. We ran the GMYC model using both a single threshold (sGMYC) and multiple threshold (mGMYC). For the bPTP, we ran 500,000 MCMC generations with a thinning of 100 and a 20% burn-in value. Lastly, because ABGD is a single-locus delimitation method, we used the ND2 locus. We conducted the ABGD analysis with a P_{min} of 0.001 and P_{max} of 0.1 using the Jukes-Cantor (JC69) model with a minimum slope increase (*X*) of 1.0.

To assess population structuring within the three *C. pubisulcus* clades, we used our multilocus nuclear dataset in the program Bayesian Phylogenetics and Phylogeography (BPP) to analyze each of the *C. pubisulcus* clades (*s.s*, Sibu, and Miri) under the multispecies coalescent model (Yang, 2015). We included this approach to estimate whether each of the respective populations were genetically distinct units, potentially warranting delineation. We utilized a reduced taxa dataset for BPP that only incorporated individuals from the three *C. pubisulcus* lineages and *C. muluensis* due to incomplete nuclear gene coverage for the ingroup. To compare clades within the *s.s.*, Sibu, and Miri lineages, we analyzed each group independently using the clades uncovered in the mtDNA tree. We then used the mitochondrial tree to designate intraspecific clades prior to running BPP (Table 2). However, we excluded the mitochondrial data from our analyses to mitigate the varying effects that introgression and selection have on autosomal and mitochondrial genes (Flouri et al., 2018). We ran the rjMCMC for 500,000 generations for each group with a burn-in period of 100,000. We used the "diploid" variable in BPP, to account for unphased sequences, and removed sites with ambiguity. We set the prior for the expected genetic divergence (θ) using an inverse-gamma (IG) distribution: $\theta \sim$ IG (3, 0.005) with a mean of (1-alpha)/beta = 0.01. We assigned an IG prior for the root height parameter $\tau \sim$ IG (3, 0.02) with a mean = 0.01. We tested the sensitivity of the species delimitation results to the prior distribution by repeating our analyses with different prior values for θ and τ. We also ran

TABLE 2 Population groupings used for Bayesian Phylogenetics and Phylogeography (BPP) species delimitation

C. "pubisulcus" lineage	No. of populations estimated	Number and assignment of input clades
West (*s.s.*)	2	1: Bau + Borneo Highlands + Kuching 2: Gunung Matang + Gunung Pueh + Gunung Gading
C. sp. nov. (Sibu)	2	1: Pelagus 2: *C. muluensis*: Gunung Mulu
C. sp. nov. (Miri)	3	1: Lawas 2: Gunung Mulu +Niah 3: Lambir Hills

Note: Number of populations estimated is based on the number of clades formed in the mitochondrial phylogeny. See Figure 1 for the geography of each clade.

the analyses without sampling the data to directly compare the prior and posterior distributions and verify that the data contained useful information for estimating parameters.

2.5 | Morphological character data

We collected morphological data to test the hypothesis that the three genetic lineages of *C. pubisulcus* are morphologically cryptic, and to examine each lineage for diagnostic features. Due to the high species richness of *Cyrtodactylus*, we focused comparisons of the morphology of our new species to the 10 Bornean congeners due to their phylogenetic placement. We examined specimens from the following collections: CAS; Field Museum of Natural History, Chicago, USA (FMNH); Osaka Museum of Natural History, Osaka, JP (OMNH), Kyoto University Museum, Kyoto, JP (KUZ), and Lee Kong Chian Natural History Museum, Singapore (ZRC). Specimens used for comparison are shown in the appendix of Davis et al. (2019) and Morphology Data S1.

The morphological measurements included in our study used to assess variation and compare the new species to their Bornean congeners are as follows: snout-vent length (SVL); tail length (TL); tail width (TW); forearm length (FL); humerus length (HU); tibia length (TBL); femur length (FE); axilla to groin length (AG); head length (HL); head width (HW); head depth (HD); eye diameter (ED); ear length (EL); eye to ear distance (EE); eye to snout distance (ES); eye to nostril distance (EN); inner orbital distance (IO); fourth front digit length (FDL); and fourth rear digit length (RDL). Meristic and other character data taken from the type series were as follows: numbers of supralabial and infralabial scales; degree of body tuberculation; presence or absence of tubercles on the dorsal and ventral margins of the forearm; number of paravertebral tubercles; presence or absence of tubercles in the gular region and ventrolateral body folds; number of longitudinal rows of dorsal tubercles; number of ventral scales; number of subdigital lamellae beneath the fourth toe (counted for the full toe and by isolating the distal and proximal phalanges); total number of femoral and precloacal pores; qualitative characteristic of the depression in the precloacal area, or lack thereof; degree and arrangement of body tuberculation; and quantity and/or quality of body bands. When possible, we took measurements from the ventral surface, and the left side of the body (specific methods of data collection in Davis et al. (2019)). To provide a qualitative assessment of precloacal area, as well as update the characterization of recognized Bornean species, we follow the precloacal descriptions provided in Mecke et al. (2016). We took morphological measurements using a Mitutoyo ^{TM} vernier caliper to the nearest 0.1 mm. In total, our dataset included 40 morphological features (Morphology Data S1).

To characterize morphometric variations within and between the cryptic species of interest in our study, we analyzed the data using a principal component analysis (PCA) with scaling and a linear discriminant analysis (LDA). We trimmed our morphological dataset to only include morphometric data that had variation among or between the species of interest. In total, our trimmed dataset included 54 specimens and 13 measurements (Morphology Data S2). We included representatives from each clade with 21 *C. pubisulcus s.s.*, eight Sibu, and 25 Miri specimens. Clade designation was determined by the locality from which the samples were collected. The LDA enabled us to determine if the morphometric data was sufficient to accurately assign species to their proper clade. We size corrected the dataset to account for allometric growth (Lleonart et al., 2000). To do so, we ran a linear regression for each included body part against the SVL to extract the unstandardized regression coefficient. We then subtracted the coefficient from the unadjusted data to get the size corrected value for each character (Thorpe, 1983). To further avoid the effects of allometry, we restricted analyses to adult individuals with a SVL of at least 60 mm. All analyses were conducted using RStudio v.1.1.4.

2.6 | Ancestral state estimation

We provide an a posteriori hypothesis about conserved morphology in *Cyrtodactylus* in attempt to conceptualize the factors contributing to the noted cryptic morphology. To gain a better understanding of the ancestral form of the *Cyrtodactylus* genus, we assembled a mitochondrial dataset of all *Cyrtodactylus* species with published *ND2* sequences. We inferred the tree using IQ-TREE with UFBs. Our dataset included sequences for 149 taxa, representing 144 species of *Cyrtodactylus* from across their geographic range. We included more than one individual for *C. pubisulcus s.s.*, *C.* sp. nov. Miri, and *C. consobrinus* to account for the high intraspecific pairwise distance within these groups (Davis et al., 2020). To estimate the ancestral state of the Bornean species, we used a Bayesian approach in the R package "phytools" (Revell, 2012). Each species was assigned to one of the five groups: (1) medium-sized rock dwelling, dark bands with white outlines; (2) medium-sized rock dwelling, banded with light interspersing bands; (3) small to medium-sized forest dwelling, often blotchy; (4) large-bodied forest dwelling, often banded; (5) species that do not fit

these generalized patterns. All morphology and natural history data used for designated groups was derived from the original description material.

3 | RESULTS

3.1 | Phylogenetic relationships

The concatenated ML and Bayesian topologies were concordant across the majority of nodes, despite both lacking support for the deeper relationships (Figures 2 and S1; Tree Files S1-S2). The placement of *C.* sp. nov. Miri differs between the two analyses, although both topologies have weak nodal support (UFB 66; PP = 0.47). The Bayesian topology places the species as sister to the Philippine clade comprising *C. philippinicus*, *C. agusanensis*, *C. mamanwa*, *C. gubaot*, and *C. sumuroi* (Figure 2); whereas the ML topology places *C.* sp. nov. Miri as sister to all recognized Bornean and Philippine lineages other than *C. consobrinus*, *C. malayanus*, and *C. limajalur*, which arose from a separate invasion of Borneo from mainland Sundaland (Davis et al., 2020). The placement of *C.* sp. nov. Miri is weakly supported in both topologies. We also compared the single locus mitochondrial and nuclear topologies, which consistently infer a non-monophyletic relationship for *Cyrtodactylus* "*pubisulcus*." Topological discordance is present between the various analyses, yet due to the non-overlapping nuclear datasets for Bornean and Philippine taxa, we are unable to accurately compare the discordant topologies (Figure S1). Despite discordant topologies between some analyses, all inferences recover *C. pubisulcus* as a polyphyletic group, indicating that the species name has been applied to at least three independent species.

3.2 | Species delimitation

All single-locus species delimitation analyses support specific recognition for *C.* sp. nov. Sibu and *C.* sp. nov. Miri, but the models, including the multi-locus BPP analysis, varied in the estimated number of putative species ranging between five and nine. ABGD estimates the least number of species for the *C. pubisulcus* complex by estimating five species, with one *C. pubisulcus s.s.*, one Sibu, and three Miri (1: Lawas; 2: Lambir Hills; 3: Gunung Mulu + Niah) clades (Table S2); BPP and sGMYC models estimate the same six species hypothesis with *C. pubisulcus* being comprised of two *C. pubisulcus s.s.* (1: Bau +Borneo Highlands and Kuching; 2: Gunung Matang; Gunung Pueh; Gunung Gading), one Sibu, and three Miri (1: Lawas; 2: Lambir Hills; 3: Gunung Mulu + Niah) clades. The PTP model estimates seven species, with three *C. pubisulcus s.s.* (1: Kuching; 2: Bau + Borneo Highlands; 3: Gunung Matang + Gunung Pueh), one Sibu, and three Miri (1: Lawas; 2: Lambir Hills; 3: Gunung Mulu + Niah) clades. mGMYC estimated the highest number of species for the *C. pubisulcus* complex with nine putative species comprising five *C. pubisulcus s.s.* (1: Borneo Highlands; 2: Kuching; 3–4: Bau; 5: Gunung Matang; Gunung Pueh; Gunung Gading), two Sibu (1–2: Pelagus), and two Miri (1: Gunung Mulu + Lawas; 2: Lambir Hills; Figure 2) clades.

Our results provide strong support against *C. pubisulcus* being a single conspecific lineage spanning Sarawak and Sabah. Using the deep phylogenetic divergences (Tables S3–S5; Davis et al., 2020), geographic separation, and minor morphometric differences among the three lineages, we formally recognize the Sibu and Miri lineages below.

3.3 | Morphological analyses

The three polyphyletic *Cyrtodactylus* "*pubisulcus*" lineages (*s.s.*, Sibu, Miri) demonstrate a high degree of intraspecific variation, resulting in overlap of morphological features and color patterns among the three lineages (Figure 3; taxonomy below). Diagnostic characters that are often used to delineate *Cyrtodactylus* species showed a high level of variation, with substantial disparity in the number of ventral scales, precloacal pores, and tuberculation, and no femoral pores, enlarged femoral scales, or variation in the type of precloacal depression. Including all specimens that genetically cluster with one of the three lineages, *C. pubisulcus s.s.* can vary from 5–10 precloacal pores (N = 16), whereas Sibu (N = 2) and Miri (N = 16) range from 0–6 and 0–9 precloacal pores in adult males, respectively. We cannot, however, confidently state that *C.* sp. nov. Sibu has a maximum of six precloacal pores because only two male specimens were available for examination.

To visualize the region of morphospace that each species fills, we conducted a PCA and LDA. The PCA demonstrates minimal differences between the three lineages with substantial overlap (Figure 4), with principal components (PC) 1–3 being the most informative. The most variation in the PCA is explained by PC1 at 36%, PC2 accounts for 11%, and PC3 accounts for 9% (Table S6). The LDA shows greater distinction between each of the three clades, although a high amount of overlap is shown between the groups. The morphological species assignment called using principal components in the LDA is shown in Table 3. *Cyrtodactylus pubisulcus s.s.* species assignment is the most inconsistent with only 71% of specimens being properly assigned to their respective genetic group. *Cyrtodactylus* sp. nov. Sibu is accurately assigned 87.5% of the time, yet the small sample size of eight individuals brings to question whether additional individuals could be assigned with similar accuracy. *Cyrtodactylus* sp. nov. Miri is most consistently assigned to the correct genetic group with 88% of individuals being accurately placed. No single morphological character weighted particularly heavily on any of the three informative principal components.

Previous records have considered *C. pubisulcus* to be widespread, as a result many morphology records for the species include *C.* sp. nov. Miri *C.* sp. nov. Sibu. Thus, we provide an updated diagnosis for *C. pubisulcus sensu stricto* using holotype data from the original description (Inger, 1961) and specimens we collected from the type locality of Gunung Matang, Sarawak. Additionally, because of the population structure within *C.* sp. nov. Miri, the diagnosis for the species only uses specimens from the type locality of Gunung Mulu.

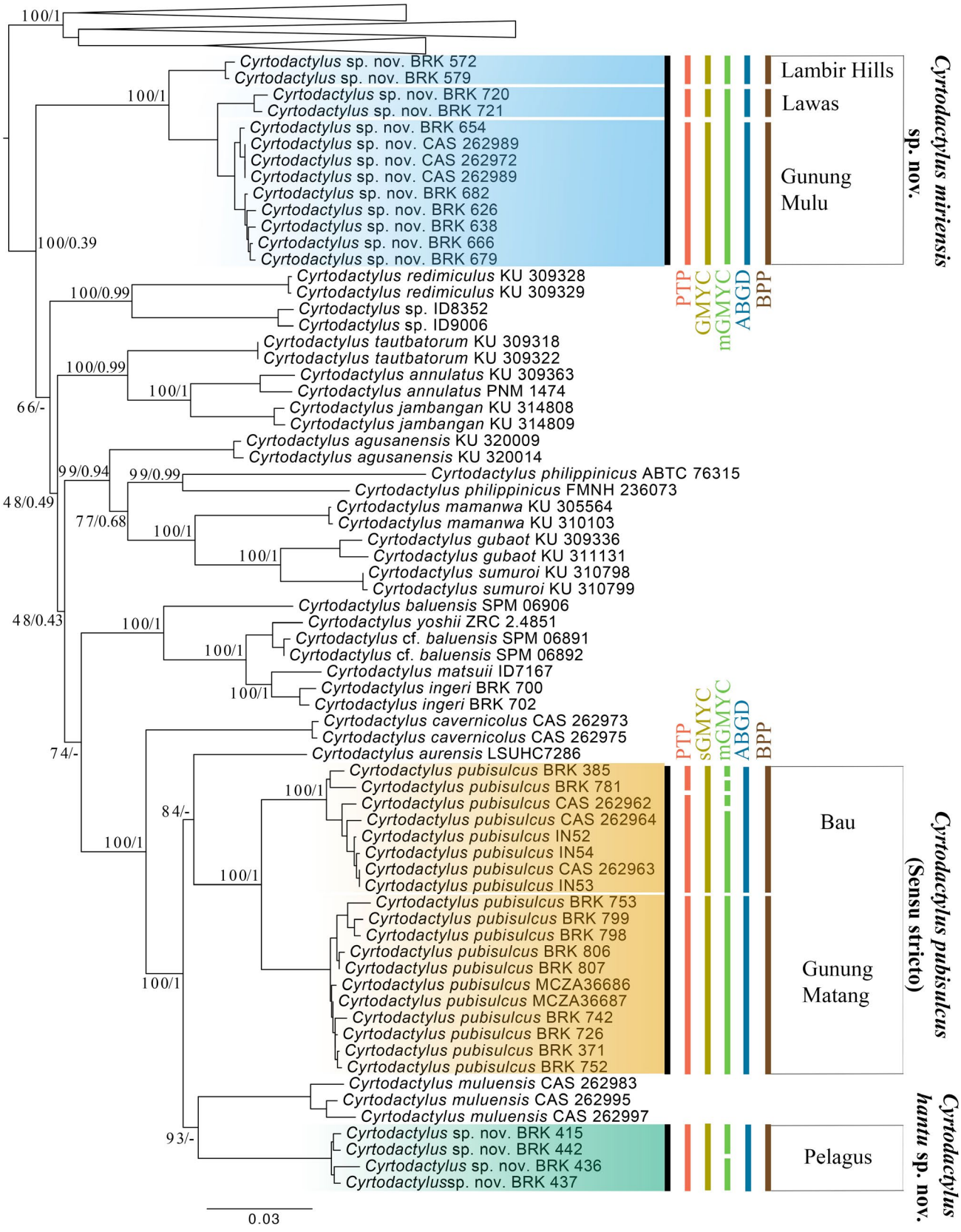

FIGURE 2 ML phylogeny highlighting the clades that are currently considered *Cyrtodactylus pubisulcus*. Values on the nodes correspond to the Bayesian posterior probability followed by the UFBoot2 values. Posterior probabilities ≥0.95 and UFB values ≥95 are considered well-supported. Partitioning schemes inferred by each of the species delimitation models are denoted by colored bars. Black bars at the end of the tip labels indicate the species delineation scheme used in this paper. Clade colors correspond to the map presented in Figure 1

FIGURE 3 Intraspecific variation and interspecific overlap in live individuals of the *Cyrtodactylus pubisulcus* complex. Upper row (a–c) *C. pubisulcus s.s.*; middle row (d–f) *C. hantu* sp. nov.; and lower row (g–i) *C. miriensis* sp. nov. Border colors correspond to the map presented in Figure 1

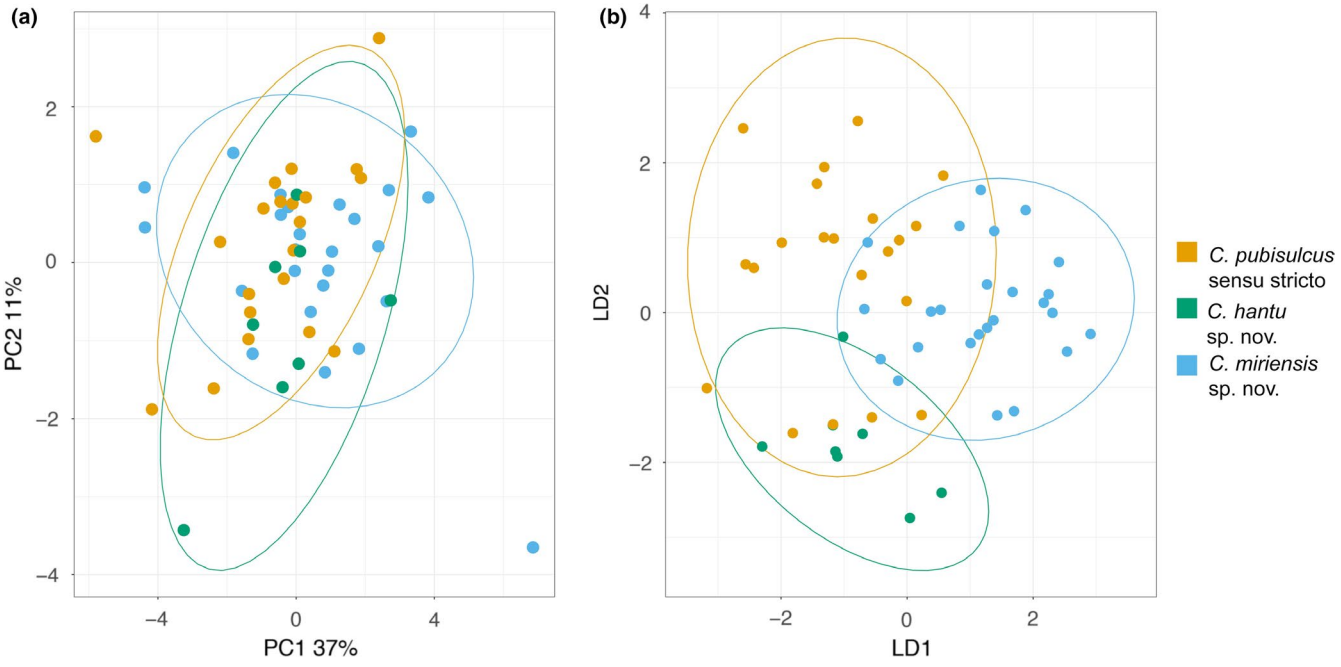

FIGURE 4 (a) Principal component analysis (PCA); and (b) linear discriminant analysis (LDA) of morphometric data for *Cyrtodactylus pubisulcus*, *C. hantu* sp. nov., and *C. miriensis* sp. nov.

TABLE 3 Morphological species assignments estimated by the linear discriminant analysis (LDA)

		Species Assignment from LDA		
		C. pubisulcus s.s.	Sibu	Miri
Genetic Species Assignment	*C. pubisulcus s.s.* (21 samples)	15	3	3
	Sibu (8 samples)	1	7	0
	Miri (25 samples)	3	0	22

Note: Rows indicate the molecular species assignment, with the total number of specimens included in parentheses; columns indicate the species assignment predicted by the LDA using morphometric data.

4 | TAXONOMY

Cyrtodactylus pubisulcus sensu stricto

Holotype (Table 4).

Adult male, FMNH 76251 collected from Gunung Matang, Kuching Division, Sarawak, East Malaysia. Collected by Robert Inger on July 26, 1956.

Paratypes

Paratypes (FMNH 76249–76250; not included in dataset) have the same collection locality but were collected on July 28, 1956. Both paratypes are juveniles and sex could not be determined.

Diagnosis (Table 4).

Cyrtodactylus pubisulcus can be distinguished from all of *Cyrtodactylus* species by a combination of the following characters: maximum SVL of at least 74 mm; 10–13 supralabials; 9–12 infralabials; weak tuberculation on dorsal surface of body; no tubercles on ventral surface of body; 46–53 paravertebral tubercles; 17–22 longitudinal tubercle rows; 37–47 ventral scales; 20–23 subdigital lamellae on fourth toe; no femoral pores; no enlarged femoral scales; 7–8 precloacal pores; precloacal slit; blotches and/or indistinct dorsal body bands; no rostral chevron; and no single row of enlarged caudal scales. The species can further be distinguished using genetic data.

Distribution (Figure 1).

Cyrtodactylus pubisulcus is known from the Kuching district of Sarawak. Specimens have been collected from Bau, Gunung Gading,

TABLE 4 Meristic, color, and measurement data for *Cyrtodactylus pubisulcus* specimens from the type locality, Gunung Matang, Kuching Division, Sarawak, Malaysia. Key to abbreviations in Materials and Methods

	FMNH 76251 *Holotype*	UNIMAS 9633	UNIMAS 9634	UNIMAS 9635	UNIMAS 9636	UNIMAS 9637	UNIMAS 9638	CAS 262968
Sex	M	M	M	F	F	F	F	M
SVL	67.2	66.6	68.0	73.6	69.3	73.9	67.0	64.0
Supralabial	10	12	13	12	12	12	10	13
Infralabial	10	10	11	9	10	10	9	12
4^{th} Toe Lamellae	23	21	21	21	21	20	21	21
Ventral Scales	N/A	37	45	37	42	47	33	42
Precloacal Pores	N/A	8	7	N/A	N/A	N/A	N/A	7
Paravertebral tubercles	N/A	55	46	49	50	48	51	53
Longitudinal tubercle rows	17–22	18	18	19	18	19	19	18
HL	N/A	17.8	19.4	20.6	18.0	19.8	18.8	17.3
HW	N/A	11.6	12.3	12.8	11.5	12.9	11.8	10.9
HD	N/A	6.9	7.0	7.6	6.9	7.9	7.1	6.3
Radius	N/A	11.3	10.6	11.3	9.8	11.3	10.6	10.3
Humerus	N/A	7.9	7.7	8.7	7.2	8.1	8.1	7.3
Tibia	N/A	11.9	12.9	13.3	11.8	13.3	12.8	11.1
Femur	N/A	11.1	11.8	12.9	11.2	12.4	11.4	10.5
EE	N/A	5.2	5.7	5.1	4.7	5.2	5.0	4.8
ES	N/A	6.7	7.5	8.1	7.3	8	7.1	7.3

FIGURE 5 Holotype of *Cyrtodactylus hantu* sp. nov. (a) Dorsal and (b) ventral view of holotype UNIMAS 9615 (BRK 415)

Gunung Mulu, Gunung Pueh, Serian, and areas within and around Kuching. However, genetic data demonstrates substantial population structure, and some of these populations may warrant elevation to full species with further studies (Figure 2). The true extent of the species distributional range is currently unknown. All individuals were observed between 30–400 m asl.

***Cyrtodactylus hantu* Davis et al., sp. nov.** (*C.* sp. nov. Sibu)

zoobank.org:act:2FD95192-F414-4B23-B5BE-5B8D90261805

Pelagus Bent-toed Gecko.

Holotype (Figure 5; Table 5).

Adult male, UNIMAS 9615 (BRK 415) collected from Pelagus Resort, Nanga Merit, Kapit Division, Sarawak, East Malaysia. (2.18576 N; 113.05753E; ~75 m asl; WGS 1984); collected by Ben Karin on June 10, 2014 at 2000–2200 hrs.

Paratypes (Figure 6; Table 5).

Paratypes UNIMAS 9616–9619 (BRK 436–439)have the same collection data as the holotype. Paratypes UNIMAS 9631 and UNIMAS 9639 (MCZ A-36673–36674) were collected from the same locality on June 10, 2018 by Hayden Davis and Izneil Nashriq.

Diagnosis.

Cyrtodactylus hantu sp. nov. can be distinguished from all of *Cyrtodactylus* species by a combination of the following characters: maximum SVL of at least 73 mm; 10–12 supralabials; 9–12 infralabials; weak tuberculation on dorsal surface of body; no tubercles on ventral surface of body; 37–48 paravertebral tubercles; 13–19 longitudinal tubercle rows; 34–46 ventral scales; 19–22 subdigital lamellae on fourth toe; no femoral pores; no enlarged femoral scales; 0–6 precloacal pores; precloacal slit; blotches, indistinct dorsal body bands, and/or longitudinal stripes; no rostral chevron; and no single row of enlarged caudal scales. The species can further be distinguished using fixed genetic differences.

Description of holotype.

Adult male; 68.3 mm SVL; 87.4 mm TL; head not much wider than body, moderate in length (HL/SVL 0.27), wide (HW/HL 0.67), slightly flattened (HD/HL 0.42), distinct from neck, triangular in dorsal profile; lores flat; frontal and prefrontal regions concave; canthus rostralis rounded; snout elongate (ES/HL 0.44), rounded in dorsal profile, slightly concave in lateral profile; eye large (ED/HL 0.25); ear opening oval, small in size (EL/HL 0.048), opening lateral; eye to ear distance greater than diameter of eye; rostral scale rectangular, divided dorsally by an inverted Y-shaped furrow, no postnasal scale; two medial internasal scales, separated by three enlarged scales forming an inverted triangle, bordered laterally by first supralabials; external nares bordered anteriorly by rostral; 11 (L/R) rectangular supralabials extending to the upturn of the labial margin, supralabials 3–6 bordered by enlarged scales, first supralabial largest, tapering abruptly just posterior to midpoint of eye; 11 (L/R) infralabials extending to the upturn of the labial margin, tapering abruptly just posterior to midpoint of eye; rostral scales weakly raised; scales on lores same size as scales on canthus rostralis, nearly double the size of scales on top of head, occiput; no tubercles on the interorbital region or bony ridge bordering the orbital rim; few small tubercles on posterior portion of occiput; transverse frontoparietal ridge; 33/39 (L/R) supraciliary scales, elongate, smooth; mental triangular, bordered laterally by first infralabials and posteriorly by left and right trapezoidal postmentals that contact medially for approximately half of their length, sutures forming

TABLE 5 Meristic, color, and measurement data of the type series for *Cyrtodactylus hantu* sp. nov. from Nanga Merit, Kapit Division, Sarawak, Malaysia. Key to abbreviations in Materials and Methods

	UNIMAS 9615 Holotype	UNIMAS 9631 Paratype	UNIMAS 96339 Paratype	UNIMAS 9616 Paratype	UNIMAS 9617 Paratype	UNIMAS 9618 Paratype	UNIMAS 9619 Paratype
Sex	M	M	F	F	F	F	F
SVL	68.2	66.4	61.0	73.2	73.0	70.5	73.2
Supralabial	11	11	12	11	10	12	10
Infralabial	11	10	9	12	11	10	11
4^{th} Toe Lamellae	21	21	19	19	20	22	21
Ventral Scales	44	34	46	39	40	46	38
Precloacal Pores	0	6	N/A	N/A	N/A	N/A	N/A
Paravertebral tubercles	37	37	42	37	43	44	48
Longitudinal tubercle rows	17	16	19	13	14	18	16
HL	18.1	18.3	16.3	19.9	19.2	18.7	18.8
HW	12.2	11.6	10.6	12.7	13.3	11.9	12.6
HD	7.6	7.0	6.3	7.8	8.2	7.3	7.8
Radius	10.5	10.3	9.2	10.6	10.9	10.0	10.7
Humerus	8.8	7.5	7.1	8.5	8.5	8.7	8.8
Tibia	12.4	11.6	10.7	12.9	12.5	12.3	12.7
Femur	12.4	10.6	9.6	12.5	12.2	12.6	12.8
EE	5.3	5.4	4.1	5.1	4.9	5.1	5.6
ES	8.0	7.7	6.6	8.6	8.0	7.8	8.0

a Y-shape; double row of slightly enlarged chinshields on left, single row on right, elongate, extending posteriorly to sixth infralabial scale; and small, flat gular scales with abrupt transition to larger, flat, smooth pectoral and ventral scales.

Body with distinct, tuberculate ventrolateral folds; dorsal scales small, granular interspersed with low, regularly arranged tubercles; small intervening tubercles occasionally present; tubercles extend from top of head to caudal constriction, and onto anterior one-fifth of tail; tubercles on occiput and nape small, those on posterior portion of body largest; approximately 17 longitudinal rows of tubercles between but not including ventrolateral fold tubercles; 42 paravertebral tubercles; 44 flat imbricate ventral scales between ventrolateral body folds; ventral scales larger than dorsal scales; and precloacal scales smooth, slightly larger than ventral scales.

Forearms relatively short (FL/SVL 0.15); scales on preaxial surface of forelimbs small, tubercles absent; scales on postaxial surface flat, non-overlapping, tubercles absent; palmar scales weakly rounded; digits well developed, inflected at basal interphalangeal joints; 18/17 (L/R) subdigital lamellae on fourth finger, rectangular, broadly expanded proximal to joint inflection, slightly expanded immediately distal to joint becoming gradually more expanded near the claw; claws well-developed, relatively short; hind limbs more robust than forelimbs, moderate in length (TBL/SVL 0.18); postaxial thigh scales flat, smooth, slightly larger than dorsal granular scales; postaxial tibial scales flat, smooth; expanded femoral scales absent; 0–6 pore-bearing precloacal scales; precloacal scales expanded surrounding moderately deep precloacal slit in which pore-bearing scales are absent; plantar scales slightly raised; digits well developed, inflected at basal, interphalangeal joints; and 21/19 (L/R) subdigital lamellae on fourth toe rectangular, broadly expanded proximal to joint inflection, slightly expanded immediately distal to joint becoming gradually more expanded near the claw.

Tail original, tapering to a point distally; dorsal scales flat, circular; no enlarged median row of transverse scales on subcaudal region; no caudal furrow; base of tail forming hemipenal swelling; and 2 (L/R) cloacal spurs on hemipenal swelling, both spurs approximately equal size.

Coloration in life.

Dorsal color of head, body, limbs, and tail brown; wide dark-brown nuchal loop that extends to the tip of the snout, edged by white line; seven dark-brown bands between nuchal loop and the posterior portion of the hindlimb insertion, each edged anteriorly and posteriorly by thin dark-brown lines; body bands wider than interspaces; limbs with light-brown band/blotch pattern; ventral portion of body bearing uniform light cream color; and tail bearing 10 dark bands separated by 11 narrower grey bands dorsally, uniform beige coloration ventrally.

Variation (Figure 6; Table 5).

Specimens from the type series of *C. hantu* sp. nov. show a high degree of intraspecific variation in coloration and meristic counts.

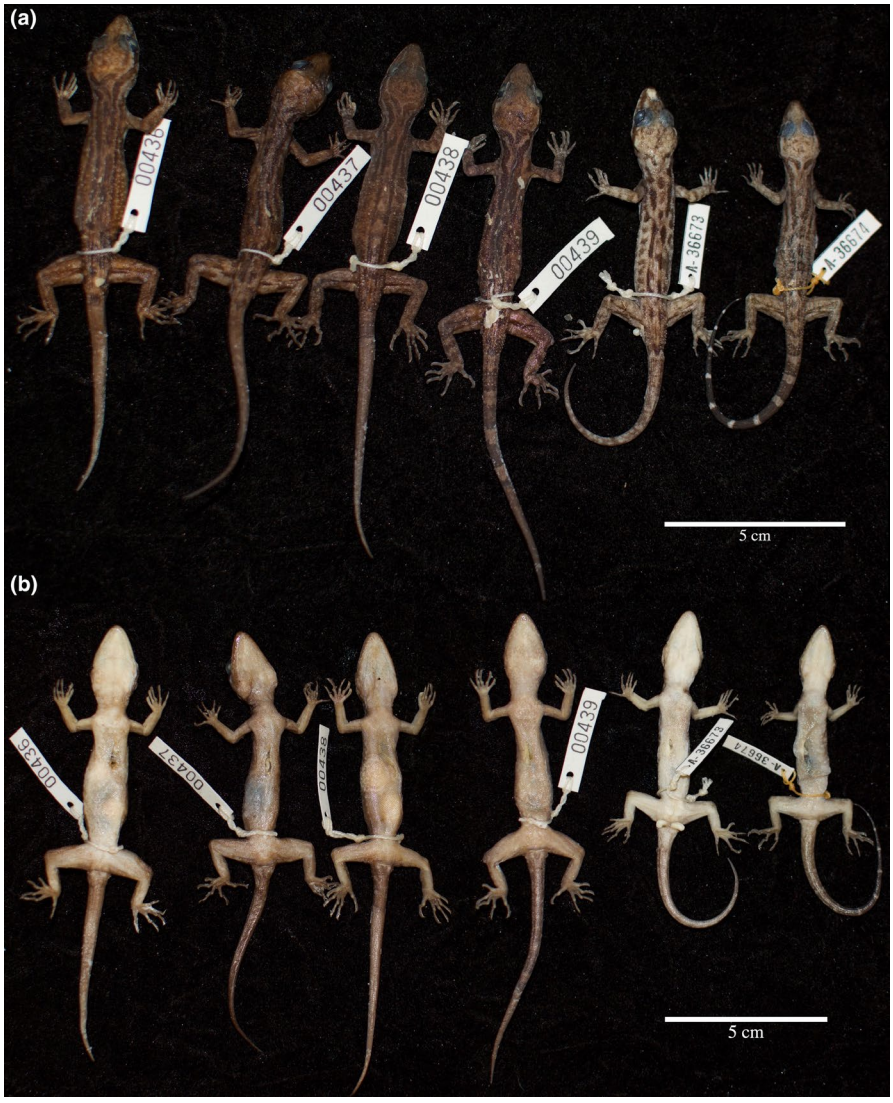

FIGURE 6 Paratypes of *Cyrtodactylus hantu* sp. nov. (a) Dorsal and (b) ventral view of the type series

The banding pattern varies with each individual, ranging from longitudinal lines to horizontal lines and blotches. The ventral scales vary from 34 (UNIMAS 9631) to 46 (UNIMAS 9618 & UNIMAS 9639); and for the two male specimens, the number of precloacal pores ranged from 0 (UNIMAS 9615) to 6 (UNIMAS 9631). The osteological measurements vary minimally when compared to SVL.

Distribution (Figure 1).

Cyrtodactylus hantu sp. nov. is known only from lowland rainforests in Nanga Merit, Kapit. The extent of the species range is currently unknown, but we expect that the species range extends beyond the forest immediately surrounding Pelagus. All specimens were observed at approximately the same elevation (75 m asl).

Etymology.

The specific epithet *hantu* is in reference to the Malay word for ghost. We chose this specific epithet for two reasons: (1) the species was found around the Pelagus Resort, a now abandoned resort in the middle of the rainforest that is said to be haunted; (2) the cryptic characteristics of this species have enabled it to hide in plain sight.

Natural history.

We collected all specimens of *Cyrtodactylus hantu* sp. nov. on low shrubs and tree branches between 0 and 1 meters from the ground. We collected all but one individual from areas with primary rainforest. We collected one semi-adult at the edge of a wooden walkway that extend from the resort. The species is nocturnal.

No other *Cyrtodactylus* species were seen in the area. We observed *Gekko monarchus* Schlegel, 1836 and *Hemidactylus frenatus* Duméril & Bibron, 1836 around the Pelagus Resort, but exclusively on building structures; *Aeluroscalabotes felinus* Günther, 1864 was found living sympatrically with *C. hantu* sp. nov.

Comparison (Table 6).

Cyrtodactylus hantu sp. nov. differs from most of their Bornean congeners by one or more morphological characteristics (Table 6). The new species is distinguished from *C. baluensis* (Mocquard, 1890) in having a precloacal slit as opposed to a pit, fewer precloacal pores (0–6 versus 9–12), and a lower number of paravertebral tubercles (37–48 versus 47–60); it is distinguished from *C. cavernicolus* Inger & King, 1961 in having fewer ventral scales (34–46 versus 51–58) and fewer subdigital lamellae on the fourth toe (19–22 versus 22–26); it is distinguished from *C. consobrinus* (Peters, 1871)

TABLE 6 Key diagnostic features for Bornean *Cyrtodactylus* species. Data for *C. pubisulcus*, *C. hantu sp. nov.*, *and C. miriensis sp. nov.* are only from specimens from the type locality

	SVL	Precloacal depression	Enlarged Femoral Scales (No.)	Preanal Pores	Subdigital Lamellae	Ventral Scales	Expanded Subcaudals	Pattern on Dorsum	Supralabial	Infralabial
C. baluensis	67–86	Pit	Y; 4–12	6–12	18–23	33–46	Y	BD	9–13	9–10
C. cavernicolus	64–81	Slit	N	4	22–26	51–58	N	BD	9–10	10
C. consobrinus	97–125	Pit	Y; 0–6	9–10	22–28	58–71	Y	BD	10–16	9–13
C. ingeri	65–76	Pit	N	8–9	23–29	40–43	Y	BD/BL	10–12	9–10
C. limajalur	73–94	Pit	Y; 5–6	7	19–22	31–38	Y	BD	12–13	9–10
C. malayanus	70–83	Pit	N	8–10	21–23	58–62	Y	BD	9–11	10
C. matsuii	89–101	Pit	Y;12–16	7–11	20–25	44–51	N	BD/BL	9–12	9–10
C. muluensis	82–88	Slit	N	4–5	19–20	31–38	Y	BD	9–13	8–12
C. pubisulcus	64–74	Slit	N	7–8	20–23	33–47	N	BL/BL	10–13	9–12
C. yoshii	75–96	Pit	N	5–12	21–30	42–58	Y	BL	10–13	9–11
C. hantu sp. nov.	61–73	Slit	N	0–6	19–22	34–46	N	BL/LB	10–12	9–12
C. miriensis sp. nov.	61–71	Slit	N	0–5	17–21	33–45	N	BL/LB	10–14	10–11

Note: Data for *C. pubisulcus*, *C. hantu* sp. nov., and *C. miriensis* sp. nov. are only from individuals from their respective type localities. Enlarged femoral scales and preanal pore values are only taken from male specimens.

Abbreviations: BD, bands; BL, blotches; LB, longitudinal bands.

in having a smaller maximum SVL (73 mm versus 125 mm), no reticulated pattern on the parietal, and a precloacal slit as opposed to a pit; it is distinguished from *C. ingeri* Hikida, 1990 in having a precloacal slit as opposed to a pit, fewer subdigital lamellae (19–22 versus 23–27), and ventral scales slightly imbricate as opposed to non-overlapping; it is distinguished from *C. limajalur* Davis et al., 2019 in having a smaller maximum SVL (73 mm versus 94 mm), no enlarged femoral scales as opposed to 5–6, and a precloacal slit as opposed to a pit; it is distinguished from *C. malayanus* (de Rooij, 1915) in having a lower number of ventral scales (34–46 versus 58–62), a smaller maximum SVL (73 mm versus 83 mm), and no reticulated pattern on the parietal; it is distinguished from *C. muluensis* Davis et al., 2019 in having a varied color pattern with dark blotches as opposed to bands, fewer precloacal pores (0–6 versus 4–5), and a smaller maximum SVL (73 mm versus 88 mm); it is distinguished from *C. matsuii* Hikida, 1990 in having a smaller SVL (73 mm vs. 105 mm) and no single row of enlarged subcaudals; and it is distinguished from *C. yoshii* Hikida, 1990 in having a smaller maximum SVL (73 mm versus 96 mm), fewer subdigital lamellae on the fourth toe (19–22 versus 25–30), and fewer ventral scales (34–46 versus 50–58). Comparisons to *C.* sp. nov. Miri and *C. pubisulcus s.s.* are provided below.

***Cyrtodactylus miriensis* Davis et al., sp. nov.** (*C.* sp. nov. Miri)

zoobank.org:act:7741F978-7182-4C56-8C40-ADD10ED70F34

Miri Bent-toed Gecko

Holotype (Figure 7; Table 7).

Adult male, CAS 262994 collected from Gunung Mulu National Park, Miri Division, Sarawak, East Malaysia. (4.02620 N; 114.82412E; ~115 m asl; WGS 1984), collected by Izneil Nashriq and Hayden Davis on July 21, 2017 at 2000–2200 hrs.

Paratypes (Figure 8; Table 7).

All paratypes were collected from the same locality as the holotype. Paratype CAS 262989 was collected by the same individuals and on the same date as the holotype; UNIMAS 9620 (BRK 572) was collected by Benjamin Karin in June 2014; UNIMAS 9621 (BRK 626) and UNIMAS 9622–9623 (BRK 654–655) were collected by Benjamin Karin in July 2015.

Diagnosis.

Cyrtodactylus miriensis sp. nov. can be distinguished from all of *Cyrtodactylus* species by a combination of the following characters: maximum SVL of at least 71 mm; 10–14 supralabials; 10–11 infralabials; weak tuberculation on dorsal surface of body; no tubercles on ventral surface of body; 47–57 paravertebral tubercles; 12–20 longitudinal tubercle rows; 33–45 ventral scales; 17–21 subdigital lamellae on fourth toe; no femoral pores; no enlarged femoral scales; 1–5 precloacal pores; precloacal slit; blotches, indistinct dorsal body bands, and/or longitudinal stripes; no rostral chevron; and no single row of enlarged caudal scales. The species can further be distinguished using fixed genetic differences.

Description of holotype.

Adult male; 61.0 mm SVL; 64.6 mm TL; head not much wider than body, moderate in length (HL/SVL 0.27), wide (HW/HL 0.67), slightly flattened (HD/HL 0.42), distinct from neck, triangular in dorsal profile; lores slightly rounded; frontal and prefrontal regions concave; canthus rostralis rounded; snout elongate (ES/HL 0.44), rounded in dorsal profile, slightly concave in lateral profile; eye large (ED/HL 0.25); ear opening triangular, small in size (EL/HL 0.048), opening lateral; eye to ear distance greater than diameter of eye; rostral scale forming "V" shape, divided dorsally by an inverted Y-shaped furrow, postnasal scales absent; two medial internasal scales, separated by one enlarged scale the base of the rostral Y-shaped furrow, bordered laterally by first supralabials; external nares bordered anteriorly by rostral, anterior and medial to first supralabial; 14/12 (L/R) rectangular supralabials extending to the upturn of the labial margin, supralabials 3–6 bordered by enlarged scales, first supralabial largest, tapering abruptly directly just posterior to midpoint of eye; 10/9 (L/R) infralabials extending to the upturn of the labial margin, tapering abruptly just posterior to midpoint of eye; rostral scales weakly raised; scales on lores same size as scales on canthus rostralis, nearly double the size of scales

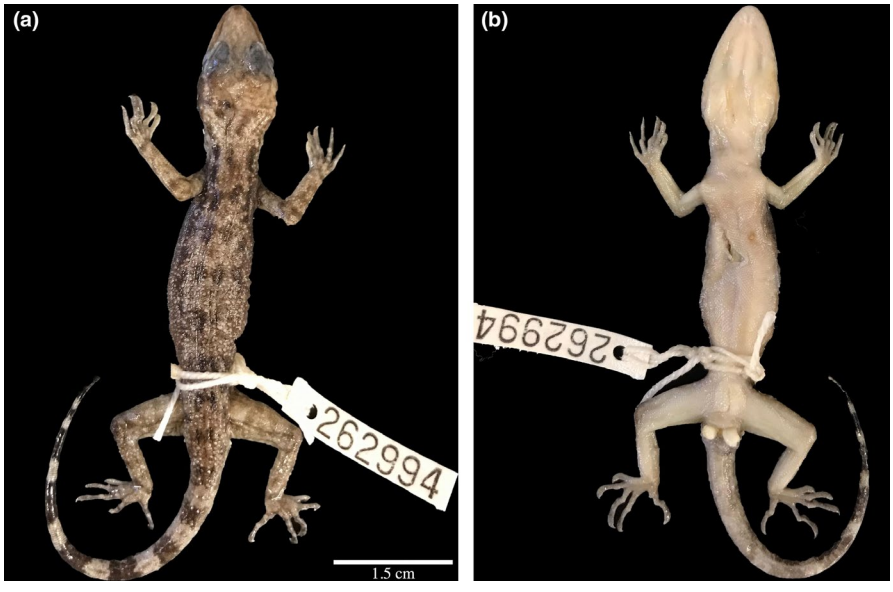

FIGURE 7 Holotype of *Cyrtodactylus miriensis* sp. nov. (a) Dorsal and (b) ventral view of holotype CAS 262994

TABLE 7 Meristic, color, and measurement data of the type series for *Cyrtodactylus miriensis* sp. nov. from Gunung Mulu, Miri Division, Sarawak, Malaysia. Key to abbreviations in Materials and Methods

	CAS 262994 Holotype	UNIMAS 9620 Paratype	UNIMAS 9621 Paratype	UNIMAS 9622 Paratype	UNIMAS 9623 Paratype	CAS 262989 Paratype
Sex	M	F	M	M	M	M
SVL	61.0	70.8	55.5	52.7	64.0	67.9
Supralabial	14	11	10	11	13	13
Infralabial	10	11	9	10	9	10
4^{th} Toe Lamellae	18	21	21	17	20	17
Ventral Scales	42	45	43	38	36	33
Precloacal Pores	0	N/A	0	0	1	5
Paravertebral tubercles	52	53	57	49	53	47
Longitudinal tubercle rows	19	21	17	20	20	15
HL	16.5	20.4	15.9	14.1	17.9	18.8
HW	10.0	12.8	10.5	9.0	10.9	11.9
HD	6.7	8.8	5.8	5.3	7.0	7.4
Radius	10.0	12.3	8.7	7.6	9.8	10.5
Humerus	7.7	10.6	6.7	6.7	7.4	8.4
Tibia	11.4	13.5	10.0	9.2	11.4	12.0
Femur	10.4	13.0	8.0	8.1	10.4	10.4
EE	3.8	5.7	4.4	2.7	4.1	4.5
ES	6.9	8.1	6.2	5.8	7.3	7.9

on top of head, occiput; no tubercles in interorbital region or bony ridge bordering the orbital rim; few small tubercles on posterior portion of occiput; indistinct frontoparietal ridge; 37/37 (L/R) distinct supraciliary scales, elongate, smooth; mental triangular, bordered laterally by first infralabials and posteriorly by left and right trapezoidal postmentals that contact medially for approximately 1/3 of their length, sutures forming a Y-shape; single row of slightly enlarged, elongate chinshields extending posteriorly to sixth infralabial scale; small, raised gular scales with abrupt transition to larger, flat, smooth pectoral and ventral scales.

Body with fairly distinct, tuberculate ventrolateral folds; dorsal scales small, granular interspersed with low, regularly arranged tubercles; small intervening tubercles occasionally present; tubercles extend from top of frontoparietal ridge to caudal constriction, and onto anterior one-fifth of tail; tubercles on nape slightly smaller than dorsum, tubercles on occiput small, those in middle of dorsum largest; approximately 19 longitudinal rows of tubercles between but not including ventrolateral fold tubercles; 52 paravertebral tubercles; 42 small, flat, slightly imbricate ventral scales between ventrolateral body folds, taken just posterior to the incision used to extract liver tissue; ventral scales larger than dorsal scales; and precloacal scales smooth, slightly larger than ventral scales.

Forearms relatively short (FL/SVL 0.15); scales on preaxial surface of forelimbs small, raised, tubercles absent; scales on postaxial surface flat, non-overlapping, tubercles absent; palmar scales weakly rounded; digits well developed, inflected at basal interphalangeal joints; 18/17 (L/R) subdigital lamellae on fourth finger, rectangular, broadly expanded proximal to joint inflection, slightly expanded immediately distal to joint becoming gradually more expanded near the claw; claws well-developed, relatively short; hind limbs more robust than forelimbs, moderate in length (TBL/SVL 0.18); postaxial thigh scales flat, smooth, slightly larger than dorsal granular scales; postaxial tibial scales flat, smooth; tubercles on preaxial portion (dorsal); expanded femoral scales absent; femoral pores absent; 0–9 pore-bearing precloacal scales; precloacal scales expanded surrounding moderately shallow precloacal slit; plantar scales slightly raised; digits well developed, inflected at basal, interphalangeal joints; and 818/17 (L/R) subdigital lamellae on fourth toe rectangular, broadly expanded proximal to joint inflection, slightly expanded immediately distal to joint becoming gradually more expanded near the claw.

Tail original, tapering to a point distally; dorsal scales flat, circular; no enlarged median row of transverse scales on subcaudal region; no caudal furrow; base of tail forming hemipenal swelling; 3 (L/R) cloacal spurs on hemipenal swelling, all spurs approximately equal size; and nine dark caudal bands interspersed with nine white spaces.

Coloration in life.

Dorsal color of head, body, limbs, and tail brown; wide dark-brown nuchal loop that extends to the tip of the snout, edged by white line; seven dark-brown bands between nuchal loop and the

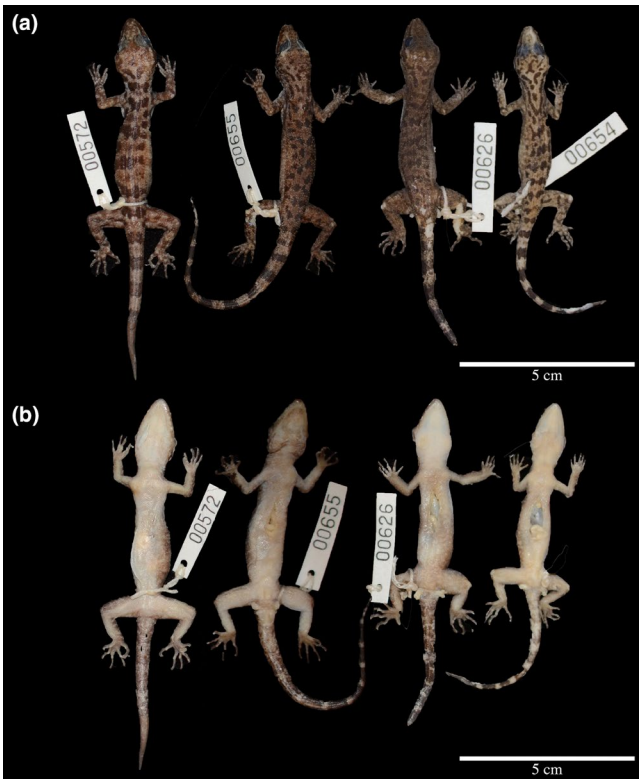

FIGURE 8 Paratypes of *Cyrtodactylus miriensis* sp. nov. (a) Dorsal and (b) ventral view of the type series. Paratype CAS 262989 not included in figure

posterior portion of the limb insertion, each edged anteriorly and posteriorly by thin dark-brown lines; body bands wider than interspaces; limbs with light-brown band/blotch pattern; ventral portion of body uniform light cream color; tail bearing 10 dark bands separated by 11, narrower grey bands dorsally, uniform beige ventrally.

Variation (Figure 8; Table 7).

Specimens in the type series of *C. miriensis* sp. nov. show a high degree of intraspecific variation in coloration and meristic counts. The banding pattern varies with each individual, ranging from blotches with no pattern (UNIMAS 9623) to blotches that roughly form body bands (UNIMAS 9620; UNIMAS 9622). The ventral scales varied from 33 (CAS 262989) to 45 (UNIMAS 9620); the number of subdigital lamellae ranging from 17 (UNIMAS 9622) to 21 (UNIMAS 9620; UNIMAS 9621) and of the two male specimens examined the number of precloacal pores ranged from 0 (UNIMAS 9621; UNIMAS 9622; UNIMAS 9620; CAS 262994) to 5 (CAS 262989). All osteological measurements taken were minimally variable when compared to SVL. Data collected from non-type material demonstrated further variation.

Including specimens of *C. miriensis* sp. nov. from outside of the type locality contributed to the variability of the genus. Including all specimens (Morphology Data S1), the maximum number of precloacal pores increased from five to nine, the minimum number of ventral scales decreased from 33 to 30, maximum number of infralabials increased from 11 to 12, the mimum number of paravertebral tubercles decreased from 47 to 44.

Distribution (Figure 1).

Cyrtodactylus miriensis sp. nov. is known from the Miri district of Sarawak. Specimens have been collected from Niah, Lawas, Lambir Hills, and Gunung Mulu, although the type series is from Gunung Mulu. The species likely also occurs in the Nation of Brunei, as previous records indicate *Cyrtodactylus pubisulcus* in the country (Das, 2007). However, we do not have genetic data to confirm this population. *Cyrtodactylus miriensis* sp. nov. contains substantial population structure, and some of these populations might warrant elevation to full species with further studies. The true extent of the species distributional range is currently unknown. All individuals were observed between 50–150 m asl.

Etymology.

The specific epithet *miriensis* is in reference to the distribution of the species in the Miri Division of Sarawak.

Natural history.

All specimens of *Cyrtodactylus miriensis* sp. nov. were collected from low-lying shrubs and tree branches between 0 and 1 meters from the ground, and man-made wooden walkways. Individuals were observed in both primary and secondary forest. The species is nocturnal and appears relatively abundant.

Gunung Mulu serves as a hotspot for gecko diversity with at least eight species recorded over the course of this study from the lowland forests, and additional records from Das et al. (2017). We observed *Aeluroscalabotes felinus* on a low-lying tree branch, *Gekko smithii* Gray, 1842, *G. monarchus* Schlegel, 1836, *Hemidactylus frenatus*, and *H. platyurus* Schneider, 1797 on buildings within the park, *Cyrtodactylus consobrinus* on large tree trunks and occasionally on limestone-karst formations, *C. muluensis* on karst and occasionally on wooden walkways, and *Cnemaspis* sp. on karst formations. All of these species co-occur with slightly varied ecologies; however, *Cnemaspis* sp. is temporally isolated from *C. miriensis* sp. nov. Despite the high gecko diversity within the park, only *A. felinus* appears to occupy the same spatio-temporal niche as *C. miriensis* sp. nov.

Comparison to Bornean congeners (Table 6).

Cyrtodactylus miriensis sp. nov. differs from most of its Bornean congeners by one or more morphological characteristics. The new species is distinguished from *C. baluensis* (Mocquard) in having a precloacal slit as opposed to a pit and fewer precloacal pores (0–5 versus 9–12); it is distinguished from *C. cavernicolus* in having fewer ventral scales (33–45 versus 51–58) and fewer subdigital lamellae on the fourth toe (17–21 versus 22–26); it is distinguished from *C. consobrinus* (Peters) in having a smaller maximum SVL (71 mm versus 125 mm), no reticulated pattern on the parietal, and a precloacal slit as opposed to a pit; it is distinguished from *C. ingeri* Hikida in having a precloacal slit as opposed to a pit, fewer subdigital lamellae (17–21 versus 23–27), and ventral scales slightly imbricate as opposed to non-overlapping; it is distinguished from *C. limajalur* in having a smaller maximum SVL (71 mm versus 94 mm), no enlarged femoral scales as opposed to

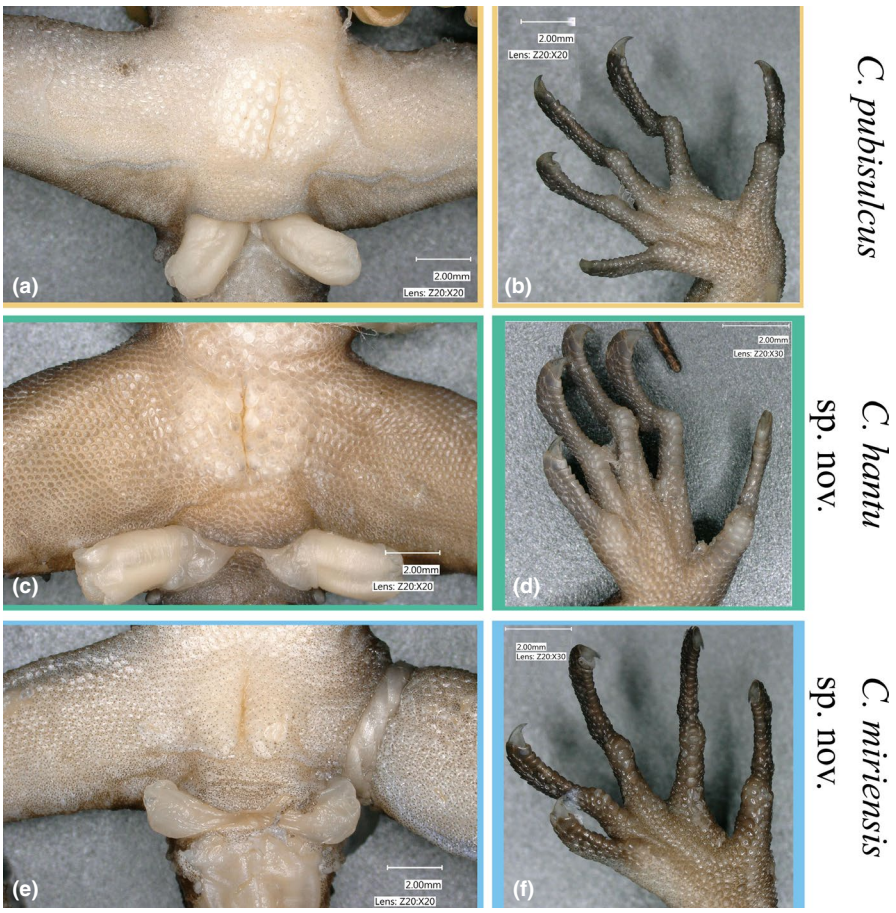

FIGURE 9 Back left foot and precloacal slit of *Cyrtodactylus pubisulcus*, *C. hantu* sp. nov., and *C. miriensis* sp. nov. (a, b) *C. pubisulcus* UNIMAS 9634 (MCZ A-36687); (c, d) *C. hantu* sp. nov. holotype UNIMAS 9615 (BRK 415); (e, f) *C. miriensis* sp. nov. paratype UNIMAS 9623 (BRK 655). Colors correspond to the map presented in Figure 1

5–6, and precloacal slit as opposed to a pit; it is distinguished from *C. malayanus* in having a lower number of ventral scales (33–45 versus 58–62), a smaller maximum SVL (71 mm versus 83 mm), and no reticulated pattern on the parietal; it is distinguished from *C. muluensis* in having a varied color pattern with dark blotches as opposed to bands, fewer precloacal pores (0–5 versus 4–5), and a smaller maximum SVL (71 mm versus 88 mm); it is distinguished from *C. matsuii* in having a smaller SVL (71 mm versus 105 mm) and no single row of enlarged subcaudals; and it is distinguished from *C. yoshii* in having a smaller maximum SVL (71 mm versus 96 mm), fewer subdigital lamellae on the fourth toe (17–21 versus 25–30), and fewer ventral scales (33–45 versus 50–58).

Comparison among cryptic species in the C. pubisulcus complex.

No morphological characters consistently distinguish *C. miriensis* sp. nov. or *C. hantu* sp. nov. from *C. pubisulcus* (specimens examined and morphological data from the type locality, Gunung Matang, shown in Table 4). Among the most frequently used diagnostic characters for differentiating *Cyrtodactylus* species (femoral and precloacal scales/pores; subdigital lamellae (Figure 9)), the three lineages do not show distinct and non-overlapping differences. Noticeable trends separating the three lineages are seen: *C. miriensis* sp. nov. and *C. hantu* sp. nov. males can have zero precloacal pores opposed to *C. pubisulcus* which has at least five pores. All three species have a high degree of variation in dorsal coloration but *C. hantu* sp. nov. seems to express longitudinal stripes more frequently than *C. miriensis* sp. nov. or *C. pubisulcus*, yet our small sample size for *C. hantu* sp. nov. may bias this finding. *Cyrtodactylus miriensis* sp. nov. has a higher maximum number of paravertebral tubercles (47–57) than *C. pubisulcus* (41–55) and *C. hantu* sp. nov. (37–48). Considering the high amount of overlap between characters, we are precluded from providing characters that can reliably distinguish each respective species. The combination of these features can often be used to identify each species, but there is definitive genetic data to distinguish them. Using genetic differences in our ND2 alignment, *C. pubisulcus* can be differentiated from the other two species by an amino acid change at base pair position 105 from a Methionine to an Alanine; *C. miriensis* sp. nov. can be distinguished by a three nucleotide insertion at position 633, and an amino acid shift from Alanine to Leucine at position 454 (Alignment S1).

5 | DISCUSSION

5.1 | Systematics and species delimitation

Using our expanded multilocus nuclear dataset for the *Cyrtodactylus pubisulcus* complex we demonstrate that rather than being one conspecific lineage spanning Sarawak and Sabah, the complex comprises at least three distantly related species. Thus, taking an approach for

describing cryptic species similar to Jörger and Schrödl (2013), we formally recognize *C. hantu* sp. nov. and *C. miriensis* sp. nov. as distinct species based primarily on their deeply divergent polyphyletic relationships, and isolated geographic distributions. Our phylogenetic analyses support previous molecular systematic studies focusing on Bornean *Cyrtodactylus* in showing that *C. pubisulcus* is not a monophyletic group (Davis et al., 2019, 2020). All phylogenetic inferences support *C. pubisulcus*, *C. hantu* sp. nov., and *C. miriensis* sp. nov. as distinct species (Figures 4 and S1).

All of our species delimitation analyses support the recognition of *C. pubisulcus*, *C. hantu* sp. nov., and *C. miriensis* sp. nov., and furthermore suggest additional putative species may be present within *C. pubisulcus* and *C. miriensis* sp. nov. The species delimitation analyses indicate that *C. pubisulcus* sensu lato can be split into the following number of putative species: mGMYC: 9; PTP: 7; sGMYC & BPP: 6; and ABGD: 5 (Figure 4). We consider it premature to describe these lineages due to having minimal to no geographic separation between clades and insufficient population sampling between localities. With further sampling, additional genetically distinct populations may be revealed making the current phylogenetic structure less clear and potentially reduce the support for delineation. Also, the differing intraspecific clades demonstrated with the nuclear loci indicate that the lineages may be subject to evolutionary processes such as nuclear gene flow, and thus genomic data and/or additional sampling may not support delimiting the groups highlighted in Figure 4 (Chan et al., 2017; Funk & Omland, 2003; Taylor et al., 2013). Taking a genomic approach with additional population sampling will provide the data necessary to detect population dynamics and demographic histories within each species.

5.2 | Intraspecific diversity

Understanding the underlying factors driving the genetic variation within and among populations of each species will require more comprehensive phylogeographic studies. The mitochondrial and nuclear data infer at least two distinct clades within *C. miriensis* sp. nov., with one clade comprising individuals from Lawas, Gunung Mulu, and Niah and the other comprising individuals from Lambir Hills (Figures 1 and S1). We expect that expanded geographic sampling will reveal a pattern of isolation-by-distance (Wright, 1943), as the populations from Lambir Hills, Gunung Mulu, and Lawas demonstrate phylogenetic substructure on a geographic gradient. Interestingly, however, the Niah population shows no phylogenetic structure despite being geographically separated from the Gunung Mulu population. The divergences seen within the *C. pubisulcus s.s.*, may be driven by different factors. Populations from the Matang Range (type locality), Gunung Gading, and Gunung Pueh are genetically indistinguishable, despite being separated by upwards of 40 km; however, the Bau, Borneo Highlands, and Kuching populations demonstrate deep genetic divergence from the type locality of *C. pubisulcus* despite a minimum 20 km separation. There are no stark geographic barriers between any populations, apart from recent habitat fragmentation; however, there are disjunct sedimentary basins and varied mineral deposit characteristics that may act as barriers to gene flow (Breitfeld et al., 2018; Hutchinson, 2005). To gain a better understanding of the factors driving the genetic diversity, the intervening geographic areas between each of these populations need to be sampled.

5.3 | Conserved morphology across diverse lineages

Unlike many cryptic species complexes, the *C. pubisulcus* complex demonstrates a unique pattern of relationships within which the most phenotypically similar taxa are not one another's closest relatives. Although this pattern has been shown in other squamate groups (Oliver et al., 2007, 2020), most recognized cryptic species have recently diverged, indicating that the indistinguishable morphology is likely due to recent shared ancestry. For the polyphyletic *C. pubisulcus* complex, however, *C. hantu* sp. nov. is estimated to have shared a common ancestor with *C. pubisulcus* approximately 14 Mya and *C. miriensis* sp. nov. is estimated to have shared a common ancestor with *C. pubisulcus* approximately 24 Mya (Davis et al., 2020). To provide perspective into the deep divergences shown, the *ND2* p-distance between *C. muluensis* and *C. miriensis* sp. nov., two indisputably independent species that are ecologically and morphologically distinct, is 14–16%. This divergence is less than the *p*-distance present between any of the three species in this study (16–21%; Davis et al., 2020). This indicates that there may be strong niche conservatism for the *C. pubisulcus* body form, whereas varied environmental pressures may have driven the morphological divergence of *C. muluensis*.

Cyrtodactylus species bearing strong superficial resemblance to *C. pubisulcus* are seen throughout Southeast Asia, indicating that the body form and color pattern may be plesiomorphic in Borneo rather than convergent. Species such as *C. quadrivirgatus* from Peninsular Malaysia, *C. majulah* Grismer Wood, Lim, 2012 from Singapore, *C. marmoratus* Gray, 1831 from Indonesia, *C. pseudoquadrivirgatus* Rösler, Nguyen, Vu, Ngo, Zeigler, 2008 from Vietnam, *C. papuensis* Brongersma, 1934 from Papua New Guinea, to name a few, are ecologically similar with largely overlapping morphologies, based on information presented in the original descriptions (Figure 10). Although some of the species shown in Figure 10 have slightly varied habitats [i.e. swamp-dwelling (Grismer & Davis, 2018); riparian (Welton et al., 2010), etc.], they tend to fill a similar niche within their respective ecosystem. This repeated small to medium-sized forest dwelling body present throughout the *Cyrtodactylus* phylogeny may stem from repeated convergence toward a forest ecomorph. However, we hypothesize that a more parsimonious scenario is that the ancestor of the Bornean and Philippine species, excluding the clade comprising *C. consobrinus*, *C. malayanus*, and *C. limajalur*, was a small-bodied forest dweller with blotched color pattern similar to *C. pubisulcus*. This evolutionary pattern of general-bodied geckos, often with spotted or blotched coloration, giving rise to diverse clades has occurred across the greater gecko

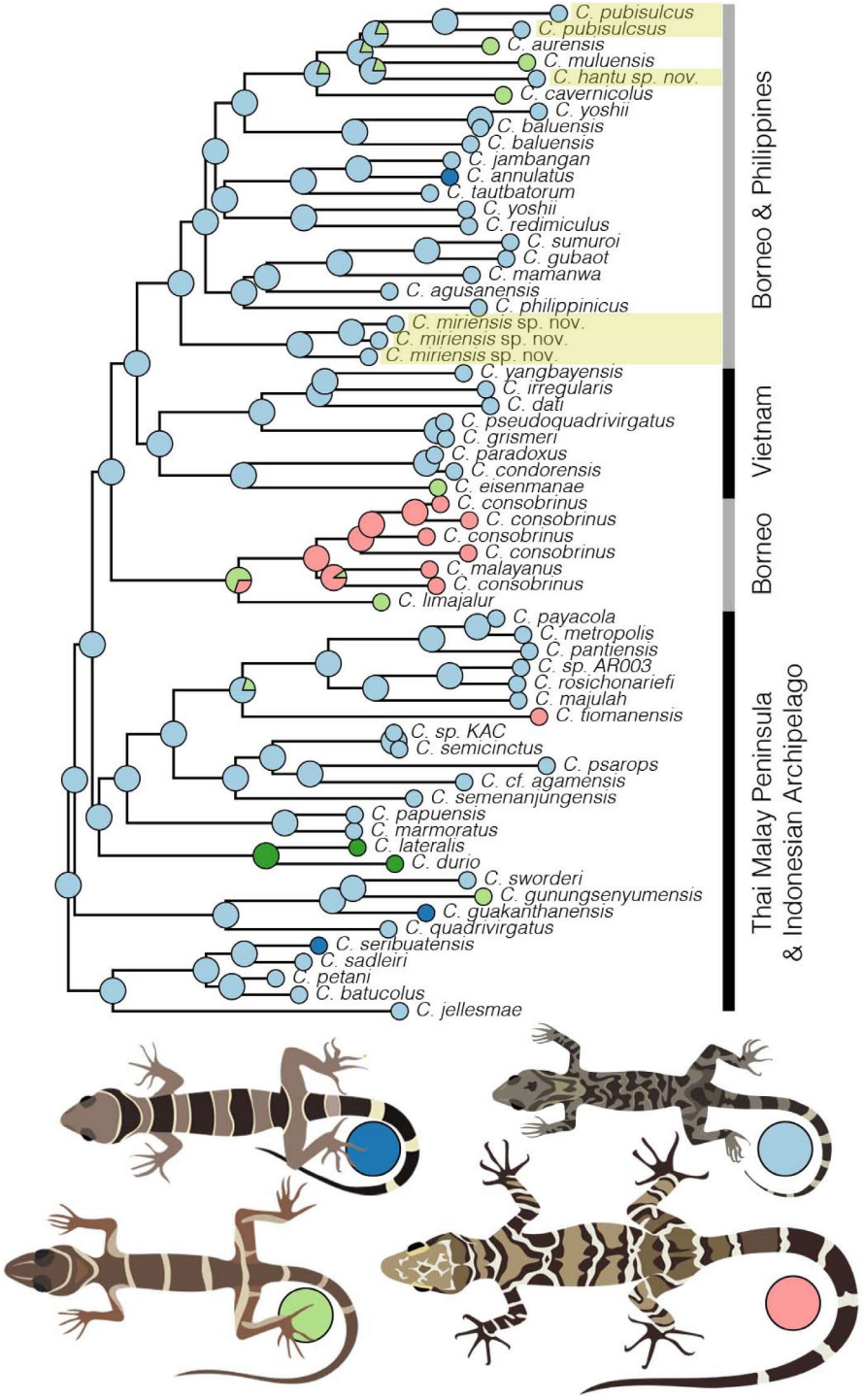

FIGURE 10 Ancestral state estimation of Bornean *Cyrtodactylus* and their closely related congeners. Ancestral estimation performed using a Bayesian approach in the the R package "phytools" (Revell, 2012) with a mitochondrial ND2 ML phylogeny as the input tree. Light green and dark blue = two banding patterns for medium-sized rock dwelling, banded; light blue = small to medium-sized forest dwelling, often blotchy; pink = large-bodied forest dwelling, often banded; dark green = species that do not fit into these generalized patterns. Focal species in this study are highlighted with a yellow box

phylogeny, including the earliest gecko lineage (Allen et al., 2019; Kulyomina et al., 2019).

Likely due to the overlapping characteristics between these species, *C. quadrivirgatus* has been recorded from Sarawak (Das, 2004, 2006; Zainudin et al., 2013), although a recent study indicated that the individuals were likely a color morph of the *C. pubisulcus* complex (Davis et al., 2020). We show additional support for *C. quadrivirgatus* being distantly related from all Bornean congeners (Figure 4). As such, we can confidently state that *C. quadrivirgatus* is restricted to the Thai-Malay peninsula and does not occur on Borneo.

5.4 | Implications of cryptic species on taxonomy

Recognizing species based primarily on molecular genetic and geographic data is not ideal, but failure to give specific recognition to *C. hantu* sp. nov. and *C. miriensis* sp. nov. propagates systematic issues for the group. Ideally, either morphological or ecological data could be used to differentiate the species to prevent future misidentifications, especially in the intermittent geographic areas that currently form the species boundaries. Despite being unable to unambiguously identify the three species, perpetuating the hypothesis that *C. pubisulcus* is one

conspecific lineage would require us to maintain a taxonomy that is not supported by the phylogeny. Further, among *Cyrtodactylus* species described in the past decade, we provide only the seventh and eighth descriptions that include nuclear data to support delineation (Table S7). With both nuclear and mitochondrial data supporting a polyphyletic relationship for the *C. pubisulcus* complex, we are confident in recognizing both *C. hantu* and *C. miriensis* as distinct species despite being unable to find morphological features that are unambiguously diagnostic.

Many recent *Cyrtodactylus* descriptions are based on minor character state differences compared across a limited number of type specimens. Using a limited number of individuals in our morphological dataset enabled us to establish putative diagnostic characters, yet those differences were not supported as more specimens were added. We expect that there are discrete differences separating *C. pubisulcus*, *C. hantu* sp. nov., and *C. miriensis* sp. nov. from one another, but we are unable to identify these with our current dataset. In an attempt to identify overlooked differences in our study, further investigations should focus on 3-D geometric morphometrics, natural history information such as pheromones, and/or behavioral differences, as these have been promising factors in identifying cryptic diversity in previous studies (Channing et al., 2002; Chaplin et al. 2020; Corl et al., 2012; Funk et al. 2012; Hebert et al., 2004; Montanarin et al., 2011; Zozaya et al., 2019).

Lastly, failure to discover and describe cryptic species undermines our biodiversity estimates and likely threatens many vulnerable lineages (Fišer et al. 2018). *Cyrtodactylus pubisulcus* has been considered a wide-ranging group but we now understand that the species is restricted to western Sarawak, and potentially further isolated to specific regions in the west. Similar phenomena have been shown for many other Bornean endemic species (Hamidy et al., 2012; Karin et al. 2016, 2018; Matsui et al., 2010; Nishikawa et al., 2012; Shimada et al., 2011). This seems to indicate that our understanding of species diversity and patterns of endemism on the island may be grossly under representative of the true biodiversity. With the high rate of deforestation and limited number of protected areas on the island, however, many of these unknown lineages may be highly vulnerable to extinction (Bryan et al., 2013; Gaveau et al., 2014). Accurate conservation assessments are predicated on correct taxonomic information and geographic ranges. As such, incorporating precise delimitation schemes and using integrative approaches to provide thorough estimates of biodiversity is imperative.

ACKNOWLEDGMENTS

The authors thank the many institutions and funding sources for the completion for this work. The authors also thank the Sarawak Forestry Department for providing collections permits [NPW.907.4.4.(Jld.14)-79; (119)JHS/NCCD/600-7/2/107]. HRD and AMB were in part funded by the Gerald M. Lemole Endowed Chair funds and Villanova University. HRD received additional funding from The Society for Integrative and Comparative Biology (Fellowship of Graduate Student Travel Award), the Museum of Comparative Zoology (Ernst Mayr Grant), and the Lee Kong Chian Natural History Museum (Collection Study Grant for Students). ID and IN were supported by a Niche Research Grant Scheme from the Ministry of Higher Education, Government of Malaysia (NRGS/1087/2013(01). We are grateful for Tsutomu Hikida (KUZ) who granted access to many specimens in the *C. pubisulcus* complex, and for the hospitality shown to HRD during data collection. Additionally, the authors thank Janneke Hille Ris Lambers and students in the course "Manuscript Writing" at the University of Washington for edits to this paper. Lastly, the authors thank Paul Oliver and two anonymous reviewers for their insightful suggestions that greatly improved the final production of this manuscript.

ORCID

Hayden R. Davis https://orcid.org/0000-0003-1401-1221

REFERENCES

Agarwal, I., & Karanth, K. P. (2015). A phylogeny of the only ground-dwelling radiation of *Cyrtodactylus* (Squamata, Gekkonidae): Diversification of *Geckoella* across peninsular India and Sri Lanka. *Molecular Phylogenetics and Evolution*, *82*, 193–199. https://doi.org/10.1016/j.ympev.2014.09.016

Agarwal, I., Mahony, S., Giri, V. B., Chaitanya, R., & Bauer, A. M. (2018). Six new *Cyrtodactylus* (Squamata: Gekkonidae) from northeast India. *Zootaxa*, *4524*(5), 501–535. https://doi.org/10.11646/zootaxa.4524.5.1

Ahmad, N., Ahmad, E., Ratag, M., Sinon, E. A. A., Don, B., Francis, F., & Belabut, D. (2019). Amphibians and reptiles of Imbak Canyon Study Centre and Batu Timbang Camp. *Journal of Tropical Biology and Conservation*, *16*, 25–33.

Aljanabi S., & Martinez, I. (1997). Universal and rapid salt-extraction of high quality genomic DNA for PCR- based techniques. *Nucleic Acids Research*, *25*(22), 4692–4693. http://dx.doi.org/10.1093/nar/25.22.4692

Allen, W. L., Moreno, N., Gamble, T., & Chiari, Y. (2019). Ecological, behavioral, and phylogenetic influences on the evolution of dorsal color pattern in geckos. *Evolution*, *74*(6), 1033–1047. https://doi.org/10.1111/evo.13915

Bauer, A. M., de Silva, A., Greenbaum, E., & Jackman, T. (2007). A new species of day gecko from high elevation in Sri Lanka, with a preliminary phylogeny of Sri Lankan *Cnemaspis* (Reptilia, Squamata, Gekkonidae). *Mitteilungen Aus Dem Museum Für Naturkunde in Berlin – Zoologische Reihe*, *83*, 22–32.

Bickford, D., Lohman, D. J., Sodhi, N. S., Ng, P. K. L., Meier, R., Winker, K., Ingram, K. K., & Das, I. (2007). Cryptic species as a window on diversity and conservation. *Trends in Ecology & Evolution*, *22*(3), 148–155. https://doi.org/10.1016/j.tree.2006.11.004

Bouckaert, R., Vaughan, T. G., Barido-Sottani, J., Duchêne, S., Fourment, M., Gavryushkina, A., Heled, J., Jones, G., Kühnert, D., De Maio, N., Matschiner, M., Mendes, F. K., Müller, N. F., Ogilvie, H. A., du Plessis, L., Popinga, A., Rambaut, A., Rasmussen, D., Siveroni, I., … Drummond, A. J. (2019). BEAST 2.5: An advanced software platform for Bayesian evolutionary analysis. *PLoS Computational Biology*, *15*(4), e1006650. https://doi.org/10.1371/journal.pcbi.1006650

Breitfeld, H. T., Hall, R., Galin, T., & BouDagher-Fadel, M. K. (2018). Unravelling the stratigraphy and sedimentation history of the uppermost Cretaceous to Eocene sediments of the Kuching Zone in West Sarawak (Malaysia), Borneo. *Journal of Asian Earth Sciences*, *160*, 200–223. https://doi.org/10.1016/j.jseaes.2018.04.029.

Brennan, I. G., Bauer, A. M., Van Tri, N., Wang, Y.-Y., Wang, W.-Z., Zhang, Y.-P., & Murphy, R. W. (2017). Barcoding utility in a mega-diverse, cross-continental genus: Keeping pace with *Cyrtodactylus* geckos. *Scientific Reports*, *7*, 1–11. https://doi.org/10.1038/s41598-017-05261-9

Bryan, J. E., Shearman, P. L., Asner, G. P., Knapp, D. E., Aoro, G., & Lokes, B. (2013). Extreme differences in forest degradation in Borneo: Comparing practices in Sarawak, Sabah, and Brunei. *PLoS One*, *8*(7), https://doi.org/10.1371/journal.pone.0069679

Carstens, B. C., Pelletier, T. A., Reid, N. M., & Satler, J. D. (2013). How to fail at species delimitation. *Molecular Ecology*, *22*(17), 4369–4383. https://doi.org/10.1111/mec.12413

Chan, K. O., Alexander, A. M., Grismer, L. L., Su, Y.-C., Grismer, J. L., Quah, E. S. H., & Brown, R. M. (2017). Species delimitation with gene flow: A methodological comparison and population genomics approach to elucidate cryptic species boundaries in Malaysian Torrent Frogs. *Molecular Ecology*, *26*(20), 5435–5450. https://doi.org/10.1111/mec.14296

Channing, A., Moyer, D., & Burger, M. (2002). Cryptic species of sharp-nosed reed frogs in the *Hyperolius nasutus* complex: Advertisement call differences. *African Zoology*, *37*(1), 91–99. https://doi.org/10.1080/15627020.2002.11657159

Chaplin, K., Sumner, J., Hipsley, C. A., & Melville, J. (2020). An integrative approach using phylogenomics and high-resolution X-ray computed tomography for species delimitation in cryptic taxa. *Systematic Biology*, *69*(2), 294–307. https://doi.org/10.1093/sysbio/syz048

Conroy, C. J., Papenfuss, T., Parker, J., & Hahn, N. E. (2009). Use of tricaine methanesulfonate (MS222) for euthanasia of reptiles. *Journal of the American Association for Laboratory Animal Science*, *48*(1), 28–32.

Corl, A., Lancaster, L. T., & Sinervo, B. (2012). Rapid formation of reproductive isolation between two populations of side-blotched lizards. *Uta Stansburiana*. *Copeia*, *2012*(4), 593–602. https://doi.org/10.1643/CH-11-166

Das, I. (2004). *Lizards of Borneo: A pocket guide*. Natural History Publications (Borneo) Sdn. Bhd.

Das, I. (2005). Bornean geckos of the genus *Cyrtodactylus*. *Gekko*, *4*(2), 11–19.

Das, I. (2006). *A photographic guide to snakes and other reptiles of Borneo* (1st ed.). New Holland Publishers (UK) Ltd.

Das, I. (2007). *Amphibians and reptiles of Brunei: A pocket guide*. Natural History Publications (Borneo) Sdn. Bhd.

Das, I., Clark, B., Clark, S., & McArthur, E. (2008). An inventory of reptiles of Gunung Mulu National Park, Sarawak, Malaysia (Borneo). *Sarawak Museum Journal*, *63*, 127–167.

Das, I., Pui, Y. M., bin Wahab, T., bin Mokhtar, S., & Zainudin, R. (2017). *A checklist of amphibians and reptiles of Gunung Mulu National Park Sarawak*. Ministry of Tourism, Culture, Youth and Sports.

Davis, H. R., Bauer, A. M., Jackman, T. R., Nashriq, I., & Das, I. (2019). Uncovering karst endemism within Borneo: Two new *Cyrtodactylus* species from Sarawak, Malaysia. *Zootaxa*, *4614*(2), 331–352. https://doi.org/10.11646/zootaxa.4614.2.4

Davis, H. R., Chan, K. O., Das, I., Brennan, I. G., Karin, B. R., Jackman, T. R., Brown, R. M., Iskandar, D. T., Nashriq, I., Grismer, L. L., & Bauer, A. M. (2020). Multilocus phylogeny of Bornean Bent-Toed geckos (Gekkonidae: *Cyrtodactylus*) reveals hidden diversity, taxonomic disarray, and novel biogeographic patterns. *Molecular Phylogenetics and Evolution*, *147*, 106785. https://doi.org/10.1016/j.ympev.2020.106785

Fišer, C., Robinson, C. T., & Malard, F. (2018). Cryptic species as a window into the paradigm shift of the species concept. *Molecular Ecology*, *27*(3), 613–635. https://doi.org/10.1111/mec.14486

Flouri, T., Jiao, X., Rannala, B., & Yang, Z. (2018). Species tree inference with BPP using genomic sequences and the multispecies coalescent. *Molecular Biology and Evolution*, *35*(10), 2585–2593. https://doi.org/10.1093/molbev/msy147

Fujisawa, T., & Barraclough, T. G. (2013). Delimiting species using single-locus data and the Generalized Mixed Yule Coalescent approach: A revised method and evaluation on simulated data sets. *Systematic Biology*, *62*(5), 707–724. https://doi.org/10.1093/sysbio/syt033

Funk, D. J., & Omland, K. E. (2003). Species-level paraphyly and polyphyly: Frequency, causes, and consequences, with insights from animal mitochondrial DNA. *Annual Review of Ecology, Evolution, and Systematics*, *34*(1), 397–423. https://doi.org/10.1146/annurev.ecolsys.34.011802.132421

Funk, W. C., Caminer, M., & Ron, S. R. (2012). High levels of cryptic species diversity uncovered in Amazonian frogs. *Proceedings of the Royal Society B: Biological Sciences*, *279*(1734), 1806–1814. https://doi.org/10.1098/rspb.2011.1653

Gaveau, D. L. A., Sloan, S., Molidena, E., Yaen, H., Sheil, D., Abram, N. K., Ancrenaz, M., Nasi, R., Quinones, M., Wielaard, N., & Meijaard, E. (2014). Four decades of forest persistence, clearance and logging on Borneo. *PLoS One*, *9*(7), e101654. https://doi.org/10.1371/journal.pone.0101654

Grismer L. L., Davis H. R. (2018). Phylogeny and biogeography of Bent-toed Geckos (*Cyrtodactylus* Gray) of the Sundaic swamp clade. *Zootaxa*, *4472*(2), 365. http://dx.doi.org/10.11646/zootaxa.4472.2.9

Grismer, L. L., & Quah, E. S. H. (2019). An updated and annotated checklist of the lizards of Peninsular Malaysia, Singapore, and their adjacent archipelagos. *Zootaxa*, *4545*(2), 230–248. https://doi.org/10.11646/zootaxa.4545.2.4

Grismer, L. L., Wood, P. L. J., Anuar, S., Grismer, M. S., Quah, E., Muin, M. A., Davis, H. R., Aguilar, C., Klabacka, R., Cobos, A. J., Aowphol, A., Murdoch, M., & Sites, J. J. (2016). Two new Bent-toed Geckos of the *Cyrtodactylus pulchellus* complex from Peninsular Malaysia and multiple instances of convergent adaptation to limestone forest ecosystems. *Zootaxa*, *4105*(5), 401–429. http://doi.org/10.11646/zootaxa.4105.5.1

Grismer, L. L., Wood, P. L., Anuar, S., Muin, M. A., Quah, E. S. H., McGuire, J. A., & Hong Thai, P. (2013). Integrative taxonomy uncovers high levels of cryptic species diversity in *Hemiphyllodactylus* Bleeker, 1860 (Squamata: Gekkonidae) and the description of a new species from Peninsular Malaysia. *Zoological Journal of the Linnean Society*, *169*(4), 849–880. https://doi.org/10.1111/zoj12064

Grismer, L. L., Wood, P. L. J., Anuar, S., Quah, E. S. H., Muin, M. A., Mohamed, M., & Heinz, H. M. (2014). The phylogenetic relationships of three new species of the *Cyrtodactylus pulchellus* complex (Squamata: Gekkonidae) from poorly explored regions in northeastern Peninsular Malaysia. *Zootaxa*, *3786*(3), 359–381. https://doi.org/10.11646/zootaxa.3786.3.6

Grismer, L. L., Wood, P. L., Thura, M. K., Zin, T., Quah, E. S. H., Murdoch, M. L., Grismer, M. S., Lin, A., Kyaw, H., & Lwin, N. (2018). Twelve new species of *Cyrtodactylus* Gray (Squamata: Gekkonidae) from isolated limestone habitats in east-central and southern Myanmar demonstrate high localized diversity and unprecedented microendemism. *Zoological Journal of the Linnean Society*, *182*(4), 862–959. https://doi.org/10.1093/zoolinnean/zlx057

Grismer, L. L., Wood, jr., P. L., Quah, E. S. H., Anuar, S., Muin, M. A., Sumontha, M., Ahmad, N., Bauer, A. M., Wangkulangkul, S., Grismer, J. L., & Pauwels, O. S. G. (2012). A phylogeny and taxonomy of the Thai-Malay Peninsula Bent-toed Geckos of the *Cyrtodactylus pulchellus* complex (Squamata: Gekkonidae): Combined morphological and molecular analyses with descriptions of seven new species. *Zootaxa*, *3520*(1), 1–55. http://dx.doi.org/10.11646/zootaxa.3520.1.1

Groth, J. G., & Barrowclough, G. F. (1999). Basal divergences in birds and the phylogenetic utility of the nuclear RAG-1 gene. *Molecular Phylogenetics and Evolution*, *12*, 115–123. https://doi.org/10.1006/mpev.1998.0603

Haile, N. S. (1974). Borneo. In A. M. Spencer (Ed.), *Mesozoic-cenozoic orogenic belts: Data for orogenic studies* (pp. 333–347). Geological Society London, Special Publication 4.

Hamidy, A., Matsui, M., Nishikawa, K., & Belabut, D. M. (2012). Detection of cryptic taxa in *Leptobrachium nigrops* (Amphibia, Anura, Megophryidae), with description of two new species. *Zootaxa*, *3398*(1), 22–39. https://doi.org/10.11646/zootaxa.3398.1.2

Hebert, P. D. N., Penton, E. H., Burns, J. M., Janzen, D. H., & Hallwachs, W. (2004). Ten species in one: DNA barcoding reveals cryptic species in the Neotropical skipper butterfly *Astraptes fulgerator*. *Proceedings of the National Academy of Sciences*, *101*(41), 14812–14817. https://doi.org/10.1073/pnas.0406166101

Heethoff, M. (2018). Cryptic species – conceptual or terminological chaos? A response to Struck et al *Trends in Ecology & Evolution*, *33*(5), 310. https://doi.org/10.1016/j.tree.2018.02.006

Hikida, T. (1990). Bornean gekkonid lizards of the genus *Cyrtodactylus* (Lacertilia: Gekkonidae) with descriptions of three new species. *Japanese Journal of Herpetology*, *13*(3), 91–107.

Hoang, D. T., Chernomor, O., Von Haeseler, A., Quang Minh, B., & Sy Vinh, L. (2017). Ufboot 2: Improving the ultrafast bootstrap

approximation. *Molecular Biology and Evolution*, *35*(2), 518–522. https://doi.org/10.5281/zenodo.854445

Hutchison, C. S. (2005). *Geology of north-west Borneo: Sarawak*, *Brunei and Sabah*. Elsevier.

Inger, R. F. (1961). A new gecko of the genus *Cyrtodactylus*, with a key to the species from Borneo and the Philippine Islands. *Sarawak Museum Journal*, *8*, 261–264.

Inger, R. F., & Tan, F. L. (2010). *The natural history of amphibians and reptiles in Sabah* (2nd ed.). Natural History Publications (Borneo).

Jörger, K. M., & Schrödl, M. (2013). How to describe a cryptic species? Practical challenges of molecular taxonomy. *Frontiers in Zoology*, *10*(1), 59. https://doi.org/10.1186/1742-9994-10-59.

Kalyaanamoorthy, S., Minh, B. Q., Wong, T. K. F., von Haeseler, A., & Jermiin, L. S. (2017). ModelFinder: Fast model selection for accurate phylogenetic estimates. *Nature Methods*, *14*(6), 587–589. https://doi.org/10.1038/nmeth.4285

Karin, B. R., Das, I., & Bauer, A. M. (2016). Two new species of diminutive leaf-litter skinks (Squamata: Scincidae: *Tytthoscincus*) from Gunung Penrissen, Sarawak, Malaysia (northern Borneo). *Zootaxa*, *4093*(3), 407–423. https://doi.org/10.11646/zootaxa.4093.3.7

Karin, B. R., Freitas, E. S., Shonleben, S., Grismer, L. L., Bauer, A. M., & Das, I. (2018). Unrealized diversity in an urban rainforest: A new species of *Lygosoma* (Squamata: Scincidae) from western Sarawak, Malaysia (Borneo). *Zootaxa*, *4370*(4), 345–362. https://doi.org/10.11646/zootaxa.4370.4.2

Katoh, K., & Standley, D. M. (2013). MAFFT multiple sequence alignment software version 7: Improvements in performance and usability. *Molecular Biology and Evolution*, *30*(4), 772–780. https://doi.org/10.1093/molbev/mst010

Kearse, M., Moir, R., Wilson, A., Stones-Havas, S., Cheung, M., Sturrock, S., Buxton, S., Cooper, A., Markowitz, S., Duran, C., Thierer, T., Ashton, B., Meintjes, P., & Drummond, A. (2012). Geneious basic: An integrated and extendable desktop software platform for the organization and analysis of sequence data. *Bioinformatics*, *28*(12), 1647–1649. https://doi.org/10.1093/bioinformatics/bts199

Koch, A., Arida, E., Schmitz, A., Böhme, W., & Ziegler, T. (2009). Refining the polytypic species concept of mangrove monitors (Squamata: *Varanus indicus* group): A new cryptic species from the Talaud Islands, Indonesia, reveals the underestimated diversity of Indo-Australian monitor lizards. *Australian Journal of Zoology*, *57*(1), 29–40. https://doi.org/10.1071/ZO08072

Korshunova, T., Picton, B., Furfaro, G., Mariottini, P., Pontes, M., Prkić, J., Fletcher, K., Malmberg, K., Lundin, K., & Martynov, A. (2019). Multilevel fine-scale diversity challenges the 'cryptic species' concept. *Scientific Reports*, *9*(1), 1–23. https://doi.org/10.1038/s41598-019-42297-5

Kulyomina, Y., Moen, D. S., & Irschick, D. J. (2019). The relationship between habitat use and body shape in geckos. *Journal of Morphology*, *280*(5), 722–730. https://doi.org/10.1002/jmor.20979

Lleonart, J., Salat, J., & Torres, G. J. (2000). Removing allometric effects of body size in morphological analysis. *Journal of Theoretical Biology*, *205*(1), 85–93. https://doi.org/10.1006/jtbi.2000.2043

Lobo, F., & Espinoza, R. E. (1999). Two new cryptic species of *Liolaemus* (Iguania: Tropiduridae) from northwestern Argentina: Resolution of the purported reproductive bimodality of *Liolaemus alticolor*. *Copeia*, *1999*(1), 122–140. https://doi.org/10.2307/1447393

Luu, V., Bonkowski, M., Nguyen, T., Le, M., Schneider, N., Ngo, H., & Ziegler, T. (2016). Evolution in karst massifs: Cryptic diversity among bent-toed geckos along the Truong Son Range with descriptions of three new species and one new country record from Laos. *Zootaxa*, *4107*(2), 101–140. https://doi.org/10.11646/zootaxa.4107.2.1

Macey, J. R., Larson, A., Ananjeva, N. B., Fang, Z., & Papenfuss, T. J. (1997). Two novel gene orders and the role of light-strand replication in rearrangement of the vertebrate mitochondrial genome. *Molecular Biology and Evolution*, *14*, 91–104. https://doi.org/10.1093/oxfordjournals.molbev.a025706

Matsui, M., Tominaga, A., Liu, W., Khonsue, W., Grismer, L. L., Diesmos, A. C., Das, I., Sudin, A., Yambun, P., Yong, H., Sukumaran, J., & Brown, R. M. (2010). Phylogenetic relationships of *Ansonia* from Southeast Asia inferred from mitochondrial DNA sequences: Systematic and biogeographic implications (Anura: Bufonidae). *Molecular Phylogenetics and Evolution*, *54*(2), 561–570. https://doi.org/10.1016/j.ympev.2009.08.003

Mayr, E. (1976). *Evolution and the diversity of life* (pp. 509–514). The Belknap Press of Harvard University Press.

Mecke, S., Kieckbusch, M., Hartmann, L., & Kaiser, H. (2016). Historical considerations and comments on the type series of *Cyrtodactylus marmoratus* Gray, 1831, with an updated comparative table for the bent-toed geckos of the Sunda Islands and Sulawesi. *Zootaxa*, *4175*(4), 343–365. https://doi.org/10.11646/zootaxa.4175.4.5

Minh, B. Q., Nguyen, M. A. T., & von Haeseler, A. (2013). Ultrafast approximation for phylogenetic bootstrap. *Molecular Biology and Evolution*, *30*(5), 1188–1195. https://doi.org/10.1093/molbev/mst024

Montanarin, A., Kaefer, I. L., & Lima, A. P. (2011). Courtship and mating behaviour of the brilliant-thighed frog *Allobates femoralis* from Central Amazonia: Implications for the study of a species complex. *Ethology, Ecology & Evolution*, *23*(2), 141–150. https://doi.org/10.1080/03949370.2011.554884

Murdoch, M. L., Grismer, L. L., Wood, P. L. J., Neang, T., Poyarkov, N. A., Tri, N. V., Nazarov, R. A., Aowphol, A., Pauwels, O. S., Nguyen, H. N., & Grismer, J. L. (2019). Six new species of the *Cyrtodactylus intermedius* complex (Squamata: Gekkonidae) from the Cardamom Mountains and associated highlands of Southeast Asia. *Zootaxa*, *4554*(1), 1–62. https://doi.org/10.11646/zootaxa.4554.1.1

Nazarov, R. A., Orlov, N. L., Sang, N. N., & Cuc, H. T. (2008). Taxonomy of naked-toe geckos *Cyrtodactylus irregularis* complex of South Vietnam and description of a new species from Chu Yang Sin Natural Park (Krong Bong District, Dac Lac Province, Vietnam). *Russian Journal of Herpetology*, *15*(2), 141–156.

Nazarov, R. A., Poyarkov, N. A., Orlov, N. L., Phung, T. M., Nguyen, T. T., Hoang, D. M., & Ziegler, T. (2012). Two new cryptic species of the *Cyrtodactylus irregularis* complex (Squamata: Gekkonidae) from southern Vietnam. *Zootaxa*, *3302*, 1–24.

Nguyen, L.-T., Schmidt, H. A., von Haeseler, A., & Minh, B. Q. (2015). IQ-TREE: A fast and effective stochastic algorithm for estimating maximum-likelihood phylogenies. *Molecular Biology and Evolution*, *32*(1), 268–274. https://doi.org/10.1093/molbev/msu300

Nguyen, S. N., Zhou, W.-W., Le, T.-N.-T., Tran, A.-D.-T., Jin, J.-Q., Vo, B. D., & Zhang, Y.-P. (2017). Cytonuclear discordance, cryptic diversity, complex histories, and conservation Needs in Vietnamese Bent-toed geckos of the *Cyrtodactylus irregularis* species complex. *Russian Journal of Herpetology*, *24*(2), 133–154. https://doi.org/10.30906/1026-2296-2017-24-2-133-154.

Nishikawa, K., Matsui, M., Yong, H.-S., Ahmad, N., Yambun, P., Belabut, D. M., Sudin, A., Hamidy, A., Orlov, N. L., Ota, H., Yoshikawa, N., Tominaga, A., & Shimada, T. (2012). Molecular phylogeny and biogeography of caecilians from Southeast Asia (Amphibia, Gymnophiona, Ichthyophiidae), with special reference to high cryptic species diversity in Sundaland. *Molecular Phylogenetics and Evolution*, *63*(3), 714–723. https://doi.org/10.1016/j.ympev.2012.02.017

Oliver, P., Hugall, A., Adams, M., Cooper, S. J. B., & Hutchinson, M. (2007). Genetic elucidation of cryptic and ancient diversity in a group of Australian diplodactyline geckos: The *Diplodactylus vittatus* complex. *Molecular Phylogenetics and Evolution*, *44*(1), 77–88. https://doi.org/10.1016/j.ympev.2007.02.002.

Oliver, P. M., Prasetya, A. M., Tedeschi, L. G., Fenker, J., Ellis, R. J., Doughty, P., & Moritz, C. (2020). Crypsis and convergence: Integrative taxonomic revision of the *Gehyra australis* group (Squamata: Gekkonidae) from northern Australia. *PeerJ*, *8*, e7971. https://doi.org/10.7717/peerj.7971

Oliver, P. M., Richards, S. J., & Sistrom, M. (2012). Phylogeny and systematics of Melanesia's most diverse gecko lineage (*Cyrtodactylus*, Gekkonidae, Squamata). *Zoologica Scripta*, *41*(5), 437–454. https://doi.org/10.1111/j.1463-6409.2012.00545.x.

Oliver, P. M., Travers, S. L., Richmond, J. Q., Pikacha, P., & Fisher, R. N. (2018). At the end of the line: Independent overwater colonizations of the Solomon Islands by a hyperdiverse trans-Wallacean lizard lineage (*Cyrtodactylus*: Gekkota: Squamata). *Zoological Journal of the Linnean Society*, *182*(3), 681–694. https://doi.org/10.1093/zoolinnean/zlx047

Ota, H., Hikida, T., Matsui, M., & Mori, A. (1992). Karyotypes of two species of the genus *Cyrtodactylus* (Squamata: Gekkonidae) from Sarawak, Malaysia. *Caryologia 45*, 43–49. https://doi.org/10.1080/00087114.1992.10797209.

Pepper, M., Doughty, P., Hutchinson, M. N., & Scott Keogh, J. (2011). Ancient drainages divide cryptic species in Australia's arid zone: Morphological and multi-gene evidence for four new species of Beaked Geckos (*Rhynchoedura*). *Molecular Phylogenetics and Evolution*, *61*(3), 810–822. https://doi.org/10.1016/j.ympev.2011.08.012

Pfenninger, M., & Schwenk, K. (2007). Cryptic animal species are homogeneously distributed among taxa and biogeographical regions. *BMC Evolutionary Biology*, *7*(121), 1–6. https://doi.org/10.1186/1471-2148-7-121

Portik, D. M., Wood, P. L., Grismer, J. L., Stanley, E. L., & Jackman, T. R. (2012). Identification of 104 rapidly-evolving nuclear protein-coding markers for amplification across scaled reptiles using genomic resources. *Conservation Genetics Resources*, *4*, 1–10. https://doi.org/10.1007/s12686-011-9460-1

Puillandre, N., Lambert, A., Brouillet, S., & Achaz, G. (2012). ABGD, Automatic Barcode Gap Discovery for primary species delimitation. *Molecular Ecology*, *21*(8), 1864–1877. https://doi.org/10.1111/j.1365-294X.2011.05239.x

Revell, L. J. (2012). phytools: An R package for phylogenetic comparative biology (and other things). *Methods in Ecology and Evolution*, *3*(2), 217–223. https://doi.org/10.1111/j.2041-210X.2011.00169.x

Rösler, H., Vu, T. N., Nguyen, T. Q., Ngo, V. T., & Zeigler, T. (2008). A new *Cyrtodactylus* (Squamata: Gekkonidae) from central Vietnam. *Hamadryad*, *33*(1), 48–63.

Sarr, A.-C., Husson, L., Sepulchre, P., Pastier, A.-M., Pedoja, K., Elliot, M., Arias-Ruiz, C., Solihuddin, T., & Aribowo, S. (2019). Subsiding Sundaland. *Geology*, *47*(2), 119–122. https://doi.org/10.1130/G45629.1

Shimada, T., Matsui, M., Yambun, P., & Sudin, A. (2011). A taxonomic study of Whitehead's torrent frog, *Meristogenys whiteheadi*, with descriptions of two new species (Amphibia: Ranidae). *Zoological Journal of the Linnean Society*, *161*(1), 157–183. https://doi.org/10.1111/j.1096-3642.2010.00641.x

Singhal, S., Hoskin, C. J., Couper, P., Potter, S., & Moritz, C. (2018). A framework for resolving cryptic species: A case study from the lizards of the Australian wet tropics. *Systematic Biology*, *67*(6), 1061–1075. https://doi.org/10.1093/sysbio/syy026

Singhal, S., & Moritz, C. (2013). Reproductive isolation between phylogeographic lineages scales with divergence. *Proceedings. Biological Sciences*, *280*(1772), 20132246. https://doi.org/10.1098/rspb.2013.2246

Skipwith, P. L., Bauer, A. M., Jackman, T. R., & Sadlier, R. A. (2016). Old but not ancient: Coalescent species tree of New Caledonian geckos reveals recent post-inundation diversification. *Journal of Biogeography*, *43*, 1266–1276. https://doi.org/10.1111/jbi.12719

Struck, T. H., Feder, J. L., Bendiksby, M., Birkeland, S., Cerca, J., Gusarov, V. I., Kistenich, S., Larsson, K.-H., Liow, L. H., Nowak, M. D., Stedje, B., Bachmann, L., & Dimitrov, D. (2018). Finding evolutionary processes hidden in cryptic species. *Trends in Ecology & Evolution*, *33*(3), 153–163. https://doi.org/10.1016/j.tree.2017.11.007

Stuart, B. L., Inger, R. F., & Voris, H. K. (2006). High level of cryptic species diversity revealed by sympatric lineages of Southeast Asian forest frogs. *Biology Letters*, *2*(3), 470–474. https://doi.org/10.1098/rsbl.2006.0505

Taylor, S. A., Anderson, D. J., & Friesen, V. L. (2013). Evidence for asymmetrical divergence-gene flow of nuclear loci, but not mitochondrial loci, between seabird sister species: Blue-Footed (*Sula nebouxii*) and Peruvian (*S. variegata*) Boobies. *PLoS One*, *8*(4), e62256. https://doi.org/10.1371/journal.pone.0062256

Thorpe, R. S. (1983). A review of the numerical methods for recognising and analysing racial differentiation. In J. Felsenstein (Ed.), *Numerical Taxonomy* (pp. 404–423). Springer.

Uetz, P. (2020). *Advanced search | The Reptile Database*. Retrieved August 17, 2020, from http://reptile-database.reptarium.cz/advanced_search.

Welton, L. J., Siler, C. D., Linkem, C. W., Diesmos, A. C., & Brown, R. M. (2010). Philippine Bent-Toed Geckos of the *Cyrtodactylus agusanensis* complex: Multilocus phylogeny, morphological diversity, and descriptions of three new species. *Herpetological Monographs*, *24*(1), 55–85. https://doi.org/10.1655/HERPMONOGRAPHS-D-10-00005.1

Wright, S. (1943). Isolation by distance. *Genetics*, *28*(2), 114–138.

Yang, Z. (2015). The BPP program for species tree estimation and species delimitation. *Current Zoology*, *61*(5), 854–865. https://doi.org/10.1093/czoolo/61.5.854

Zainudin, R., Nawan, J. U., Jopony, M. E. M., Amram, M. F., Nasip, N., Lusat, P. T., & Koon, L. C. (2013). Notes on the herpetofauna of Kampung Giam, Padawan, Sarawak. *Borneo Journal of Resource Science and Technology*, *3*(2), 47–52. https://doi.org/10.33736/bjrst.249.2013

Zhang, J., Kapli, P., Pavlidis, P., & Stamatakis, A. (2013). A general species delimitation method with applications to phylogenetic placements. *Bioinformatics*, *29*(22), 2869–2876. https://doi.org/10.1093/bioinformatics/btt499

Ziegler, T., Nazarov, R., Orlov, N., Nguyen, T. Q., Vu, T. N., Dang, K. N., Dinh, T. H., & Schmitz, A. (2010). A third new *Cyrtodactylus* (Squamata: Gekkonidae) from Phong Nha-Ke Bang National Park, Truong Son Range. *Vietnam. Zootaxa*, *2413*(1), 20–36. https://doi.org/10.11646/zootaxa.2413.1.2

Zozaya, S. M., Higgie, M., Moritz, C., & Hoskin, C. J. (2019). Are pheromones key to unlocking cryptic lizard diversity? *The American Naturalist*, *194*(2), 168–182. https://doi.org/10.1086/704059

SUPPORTING INFORMATION

Additional supporting information may be found online in the Supporting Information section.

Figure S1. Gene trees topologies for *ND2*, *MXRA5*, and *RAG1*, and a nuclear concatenated topology

Table S1. Sequences used for molecular genetic analyses

Table S2. Output for the ND2-based species delimitation method, Automatic Barcode Gap Discovery (ABGD)

Table S3. Uncorrected pairwise distances (percentages) for the nuclear locus RAG1

Table S4. Uncorrected pairwise distances (percentages) for the nuclear locus PDC

Table S5. Uncorrected pairwise distances (percentages) for the nuclear locus MXRA5

Table S6. Summary statistics for principal components analysis of morphometric data

Table S7. Type of evidence used to support delimitation of *Cyrtodactylus* species between 2010 and 2020

Alignment S1. Alignment_file.nex.

Morphology Data S1. Morphology_clean.xlsx.

Morphology Data S2. morphometric_dataset.xlsx.

Tree File S1. BEAST2.tre.

Tree File S2. iqtree.tre.

How to cite this article: Davis HR, Das I, Leaché AD, et al. Genetically diverse yet morphologically conserved: Hidden diversity revealed among Bornean geckos (Gekkonidae: *Cyrtodactylus*). *J Zool Syst Evol Res*. 2021;00:1–23. https://doi.org/10.1111/jzs.12470